

Magnesium–ibogaine therapy effects on cortical oscillations and neural complexity in veterans with traumatic brain injury

Received: 7 September 2024

Accepted: 17 June 2025

Published online: 24 July 2025

 Check for updates

A list of authors and their affiliations appears at the end of the paper

Traumatic brain injury can lead to chronic psychiatric and cognitive symptoms, coupled with changes to the nature of cortical oscillations and neural complexity. Treatment with magnesium–ibogaine was recently found to improve the sequelae of traumatic brain injury, yet the effects of ibogaine on human cortical oscillations and complexity are unknown. Resting-state electroencephalography was performed prospectively before, 3.5 days after and 1 month after magnesium–ibogaine therapy in an observational, open-label study of 30 combat veterans. We assessed the effects of ibogaine on cortical oscillations and complexity and how these neurophysiological effects relate to psychiatric and cognitive outcomes of ibogaine treatment. After treatment, slower oscillations (theta–alpha) increased in power, and power at higher frequencies (beta–gamma) decreased. Accordingly, the theta/beta ratio increased post-treatment, which correlated with improved cognitive inhibition. Peak alpha frequency and neural complexity were lower after treatment, which persisted at 1-month follow-up. These neurophysiological markers correlated with improved executive function, post-traumatic stress disorder and anxiety after ibogaine. Altogether, these findings suggest reduced spatiotemporal complexity of brain activity and ‘slowing’ of cortical oscillations in the brain at rest after magnesium–ibogaine therapy, which may relate to psychiatric and cognitive improvements after ibogaine, thus providing key insight into the effects of ibogaine on brain function in humans. Follow-up controlled clinical trials are needed to confirm the findings from this initial single-arm trial.

Traumatic brain injury (TBI) can lead to a host of psychopathologies, including but not limited to post-traumatic stress disorder (PTSD), depression, anxiety and cognitive impairment^{1,2}. First-line treatments are ineffective for many individuals who suffer from TBI-related symptoms^{3,4}. Ibogaine, an oneirogen derived from the *Tabernanthe iboga* shrub, is a promising alternative treatment for the psychiatric and cognitive sequelae of TBI. Improvements in day-to-day function, cognitive function and PTSD, depression and anxiety symptoms were recently observed after a single ibogaine treatment in veterans with a history of TBI, with effects persisting for at least 1 month^{5,6}. Despite its

therapeutic potential, the effects of ibogaine on human brain function remain largely unknown.

Cortical oscillations and neural complexity are important dimensions of brain function that appear to be perturbed after TBI^{7–12}. Neural activity commonly manifests as changes in brain rhythms, that is, cortical oscillations, which represent the large-scale interactions among many neurons. Cortical oscillations and the complexity of cortical activity serve as markers of different brain states, such as high or low arousal/alertness^{13–17}. Electroencephalography (EEG) studies have identified an association between TBI and diffuse slowing of

cortical oscillations, including findings of elevated low-frequency (delta and theta) power and theta/beta ratio, and reduced alpha power^{7–11}, as well as reduced neural complexity¹². Similarly, common sequelae of TBI, such as symptoms of PTSD, depression and anxiety, have been associated with abnormal cortical oscillations and neural complexity^{18–21}.

Understanding how cortical oscillations and neural complexity are engaged alongside improving TBI-related symptoms after ibogaine treatment is important for establishing the neurophysiological mechanisms of this promising rapid treatment. Preliminary evidence from rodent studies suggests that the administration of ibogaine can acutely decrease neural complexity and influence oscillations across delta to gamma frequency bands^{22–24}, for example, increasing theta and gamma power. However, the effects of ibogaine on human cortical oscillations and complexity have not yet been quantified. Classic psychedelic drugs, such as psilocybin, LSD (lysergic acid diethylamide) and DMT (N,N-dimethyltryptamine), have shown utility in treating psychiatric disorders such as depression²⁵ and have shown acute effects on cortical oscillations and complexity in healthy adults, such as increases in global Lempel–Ziv complexity and reductions in broadband power, which correlated with functional network integrity and subjective experiences (for example, ego-dissolution or intensity of the experience)^{26–33}. Nevertheless, ibogaine differs from these psychedelic substances in clinically and biologically meaningful ways. For example, in contrast to hallucinogenic, empathogenic and dissociative psychedelic drugs, ibogaine's distinct subjective effects are classified as oneirogenic, involving a 'dreamlike' experience with an extensive period of self-reflection. This experience includes unpleasant physical effects, enhanced memory retrieval, dreamlike visions and auditory phenomena, and a wide range of emotional and spiritual experiences (see refs. 34,35 for more information). In addition, ibogaine has a uniquely wide range of binding targets, including *N*-methyl-D-aspartate, kappa and mu opioid, and nicotinic acetylcholine receptors, and serotonin and dopamine transporters^{36,37}. How changes in cortical oscillations and neural complexity relate to the psychiatric and cognitive outcomes of treatment with ibogaine are not yet known.

Pretreatment cortical dynamics may also be useful for predicting psychiatric outcomes after ibogaine treatment. EEG is a promising tool for establishing indices of cortical dynamics as clinically deployable biomarkers due to its accessibility, affordability and sub-millisecond temporal precision. For example, pretreatment resting-state alpha power has been identified as a robust predictor of depressive symptom improvement after antidepressant pharmacotherapy³⁸. EEG predictors of ibogaine treatment outcomes have not yet been identified.

Here, as part of the prospective, single-arm study of 'magnesium–ibogaine: the Stanford traumatic injury to the CNS protocol' (MISTIC) that found striking psychiatric and cognitive improvements in Special Operations Forces veterans (SOVs) with a history of TBI⁵, we used high-density resting-state EEG to measure the effects of ibogaine treatment on cortical oscillations and neural complexity. We then sought to relate these neurophysiological mechanisms to ibogaine treatment outcomes. We hypothesized that (1) EEG measures of cortical oscillations spanning delta to gamma frequencies and Lempel–Ziv complexity would be modulated 3.5 days and 1 month after ibogaine treatment, (2) treatment-modulated brain rhythms would correlate with symptom improvement, and (3) pretreatment EEG markers would correlate with symptom improvement.

Results

Ibogaine enhances theta–alpha and reduces beta–gamma power

Linear mixed-effects models were used to assess changes in delta, theta, alpha, beta and gamma power in two predefined regions of interest (ROIs) from baseline to 3.5 days and 1 month following magnesium–ibogaine therapy (Fig. 1). *F*-statistics are reported as $F_{df1,df2}$, where *df*1

and *df*2 refer to the numerator and denominator degrees of freedom, respectively. *P*-values corrected for multiple comparisons using the false discovery rate (FDR) method are reported as P_{FDR} . Treatment had a significant effect on theta power in both ROIs (posterior: $F_{2,52} = 4.11$, $P_{FDR} = 0.033$; frontal: $F_{2,52} = 5.78$, $P_{FDR} = 0.027$) and alpha power in the posterior ROI ($F_{2,54} = 4.08$, $P_{FDR} = 0.033$; Fig. 2a). Specifically, in post hoc Dunnett's tests, theta and alpha power increased significantly post-ibogaine (posterior theta: $P = 0.014$, Cohen's $d = 0.47$; frontal theta: $P = 0.0041$, Cohen's $d = 0.61$; posterior alpha: $P = 0.021$, Cohen's $d = 0.45$). The significance of effects did not persist at 1-month follow-up ($P > 0.05$).

To explore changes in normalized power from pre- to post-ibogaine across the cortex for EEG measures that showed significant changes at the ROI level, nonparametric permutation tests were also performed in sensor and source space. In channel-wide cluster-based permutation analyses, widespread increases in theta and posterior increases in alpha power were similarly observed post-ibogaine compared with baseline (theta cluster: $P = 0.0004$; alpha cluster: $P = 0.023$; Fig. 2b). No significant clusters were identified for theta or alpha power at 1-month follow-up compared with baseline (Supplementary Fig. 1). Source estimation revealed that increases in theta power post-ibogaine were localized to bilateral fronto-central and temporal cortical regions, including regions associated with the default mode network, such as the precuneus and superior frontal cortex. Increases in alpha power were localized to parietal and occipital cortical regions, including regions associated with visual and default mode networks (Fig. 2c, Supplementary Fig. 2 and Supplementary Table 2).

Ibogaine treatment also had a significant effect on beta power in the frontal ROI ($F_{2,54} = 9.82$, $P_{FDR} = 0.0023$) and gamma power in both ROIs (posterior: $F_{2,55} = 4.16$, $P_{FDR} = 0.033$; frontal: $F_{2,55} = 4.05$, $P_{FDR} = 0.033$; Fig. 2a). In particular, frontal beta power was significantly reduced post-ibogaine ($P = 0.0001$, Cohen's $d = 0.73$), but not at 1-month follow-up ($P > 0.4$). Gamma power was significantly reduced post-ibogaine (posterior: $P = 0.025$, Cohen's $d = 0.70$; frontal: $P = 0.016$, Cohen's $d = 0.50$), which persisted at 1 month in the posterior ROI, although with a lower effect size ($P = 0.039$, Cohen's $d = 0.37$).

Congruent with the ROI-level results, channel-wide permutation analyses showed significant reductions in beta ($P = 0.002$) and gamma (cluster 1: $P = 0.001$; cluster 2: $P = 0.035$; Fig. 2b) power post-ibogaine compared with baseline, which did not persist at 1-month follow-up (Supplementary Fig. 1). This effect of increased power in slower frequencies (in the theta to alpha range) and decreased power in faster frequencies (in the beta to gamma range) post-ibogaine was similarly observed in cluster-based permutation analyses of all frequencies and channels (Extended Data Fig. 1a), with similar but mostly non-significant effects observed 1 month after treatment (Extended Data Fig. 1b). Source estimation revealed that decreases in beta and gamma power post-ibogaine were localized to bilateral frontal and temporal cortical regions, including right frontal pole and bilateral superior frontal cortex. Reductions in gamma power were additionally localized to bilateral precuneus and superior parietal cortex (Fig. 2c, Supplementary Fig. 2 and Supplementary Table 2). Furthermore, the observed effects on theta, beta and gamma power were not found in an age-matched subset of EMBARC participants after 1 week of placebo intervention. A significant increase in left parietal alpha power was observed after placebo intervention, however (see Supplementary Data 1 and Extended Data Fig. 2 for further details).

The ratio of slow versus fast oscillations was captured using theta/beta ratio, which is a putative marker of executive control³⁹. Theta/beta ratio in both ROIs was significantly changed after ibogaine treatment (posterior: $F_{2,52} = 5.87$, $P_{FDR} = 0.010$; frontal: $F_{2,52} = 4.69$, $P_{FDR} = 0.013$). Specifically, theta/beta ratio increased significantly post-ibogaine compared with baseline (posterior: $P = 0.0033$, Cohen's $d = 0.54$; frontal: $P = 0.0094$, Cohen's $d = 0.48$), which did not persist at 1-month follow-up (Fig. 3a).

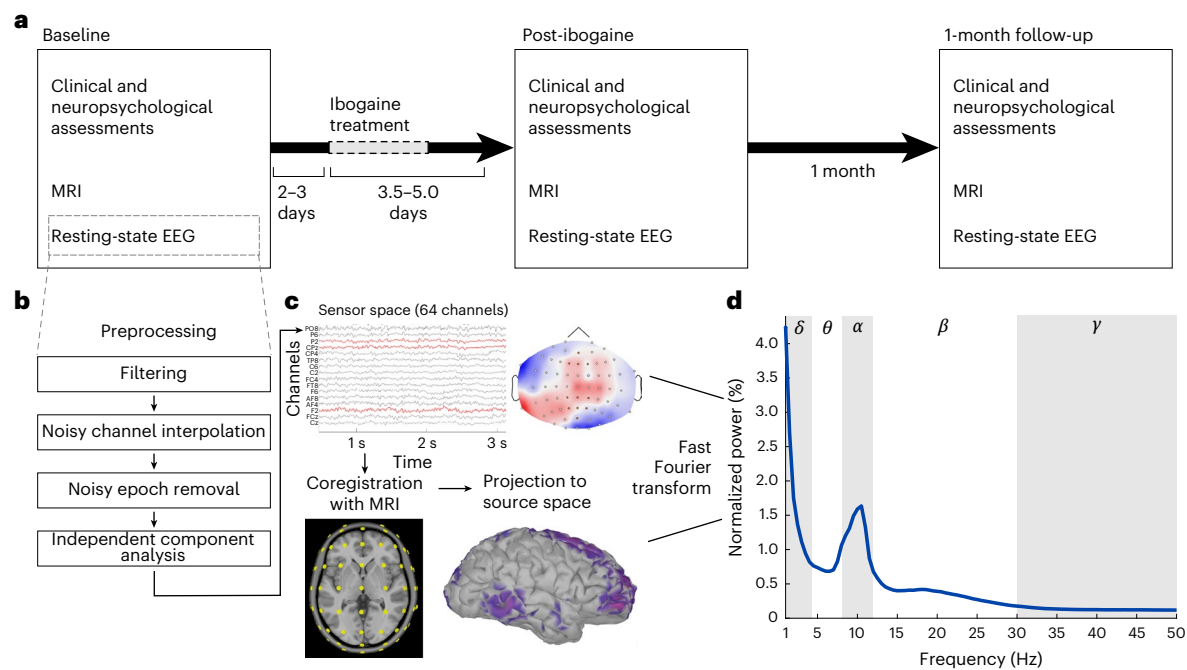


Fig. 1 | Study workflow. **a**, Timeline of data collection. Clinical and EEG data were collected at Stanford University 2–3 days before, 3.5 days after (4–5 days after for clinical assessments) and 1 month after ibogaine treatment. **b**, Resting-state EEG data from each time point were preprocessed by an experienced rater blinded to recording identifiers. **c**, Preprocessed data in sensor space

were coregistered with individual anatomical scans and projected into brain space for source localization. **d**, A fast Fourier transform was applied to the EEG data in sensor and source space to decompose cortical oscillations into their component frequencies. Power in predefined frequency bands was normalized to broadband power.

Significant decreases in delta power were also observed 1 month post-ibogaine as compared with baseline (see Supplementary Data 2 and Extended Data Fig. 3 for further details). See Supplementary Data 3 for changes in absolute power after ibogaine treatment. No significant correlations were found between total ibogaine dose or time since ibogaine administration and changes in EEG measures post-ibogaine.

Overall, the observed effects were robust in a number of sensitivity analyses, including analyses that account for the potential effects of preprocessing steps, exclude participants without a magnetic resonance imaging (MRI) scan for coregistration, exclude participants with a history of moderate to moderately severe TBI, and include alcohol consumption as a covariate (Supplementary Data 4–6). Of note, in exploratory analyses of changes in power at the online reference electrode (Cz), increased Cz theta power was observed post-ibogaine, which could have influenced the observed ROI increases in theta power post-ibogaine (see Supplementary Data 7 for further details). Importantly, most ROI EEG measures also showed excellent test–retest reliability between the two within-session EEG recordings (Supplementary Data 8 and Supplementary Table 3).

Ibogaine lowers peak alpha frequency and complexity

Global peak alpha frequency (PAF) was significantly lowered after ibogaine ($F_{2,47} = 7.38$, $P_{FDR} = 0.0024$), both post-ibogaine ($P = 0.00090$, Cohen's $d = 1.05$) and at 1-month follow-up ($P = 0.036$, Cohen's $d = 0.41$), as compared with baseline (Fig. 4). The effect of ibogaine on PAF was specific to the posterior ROI ($F_{2,47} = 8.78$, $P_{FDR} = 0.0017$), and not the frontal ROI ($F_{2,47} = 1.69$, $P_{FDR} = 0.19$). Posterior PAF was significantly reduced both post-ibogaine ($P = 0.0010$, Cohen's $d = 1.00$) and at 1-month follow-up ($P = 0.0023$, Cohen's $d = 0.56$; Fig. 4b).

Similarly, global spatiotemporal Lempel–Ziv complexity (LZc) was significantly reduced after ibogaine compared with baseline ($F_{2,55} = 4.14$, $P = 0.021$), both post-ibogaine ($P = 0.023$, Cohen's $d = 0.55$) and at 1-month follow-up ($P = 0.044$, Cohen's $d = 0.41$; Fig. 5a). These effects remained significant when LZc was normalized to LZc of

phase-randomized surrogate data (Supplementary Data 9). Temporal Lempel–Ziv complexity (LZs) was also significantly modulated after ibogaine; however these effects were not significant when phase-randomized normalization was applied (Supplementary Data 9).

Effects on aperiodic components of the signal

The ‘Fitting Oscillations and One Over F’ (FOOOF) toolbox⁴⁰ was used to explore the effects of ibogaine on aperiodic components of the EEG signal. The aperiodic offset and exponent are non-oscillatory features of the power spectra; the offset reflects uniform shifts in broadband power, and the exponent reflects the steepness of the $1/f$ slope of power across frequencies. We found significant increases in the frontal and posterior ROI aperiodic exponents (frontal: $F_{2,55} = 3.93$, $P = 0.025$; posterior: $F_{2,55} = 4.25$, $P = 0.019$), reflecting a significantly steeper $1/f$ slope post-ibogaine compared with baseline (frontal: $P = 0.020$, Cohen's $d = 0.46$; posterior: $P = 0.0072$, Cohen's $d = 0.66$), but not at 1-month follow-up (Extended Data Fig. 4). The ROI aperiodic offsets did not change significantly after treatment compared with baseline.

Changes in band power after ibogaine treatment were also analyzed with the aperiodic component subtracted from the power spectrum (Extended Data Fig. 4). In cluster-based permutation tests using the flattened power spectrum, most findings persisted: theta ($P = 0.00020$) and alpha ($P = 0.034$) power increased significantly post-ibogaine, and delta ($P = 0.020$) and gamma ($P = 0.0068$) power decreased significantly at 1-month follow-up. Similarly, significant increases in theta/beta ratio post-ibogaine compared with baseline persisted after removal of the aperiodic exponent from the spectrum (posterior: $P = 0.0032$, Cohen's $d = 0.56$; frontal: $P = 0.000042$, Cohen's $d = 0.80$). However, decreases in beta and gamma power post-ibogaine were not significant using the flattened power spectrum. In addition, with the aperiodic exponent removed, increases in theta ($P = 0.019$) and alpha ($P = 0.0086$) power were also significant at 1-month follow-up in cluster-based permutation tests.

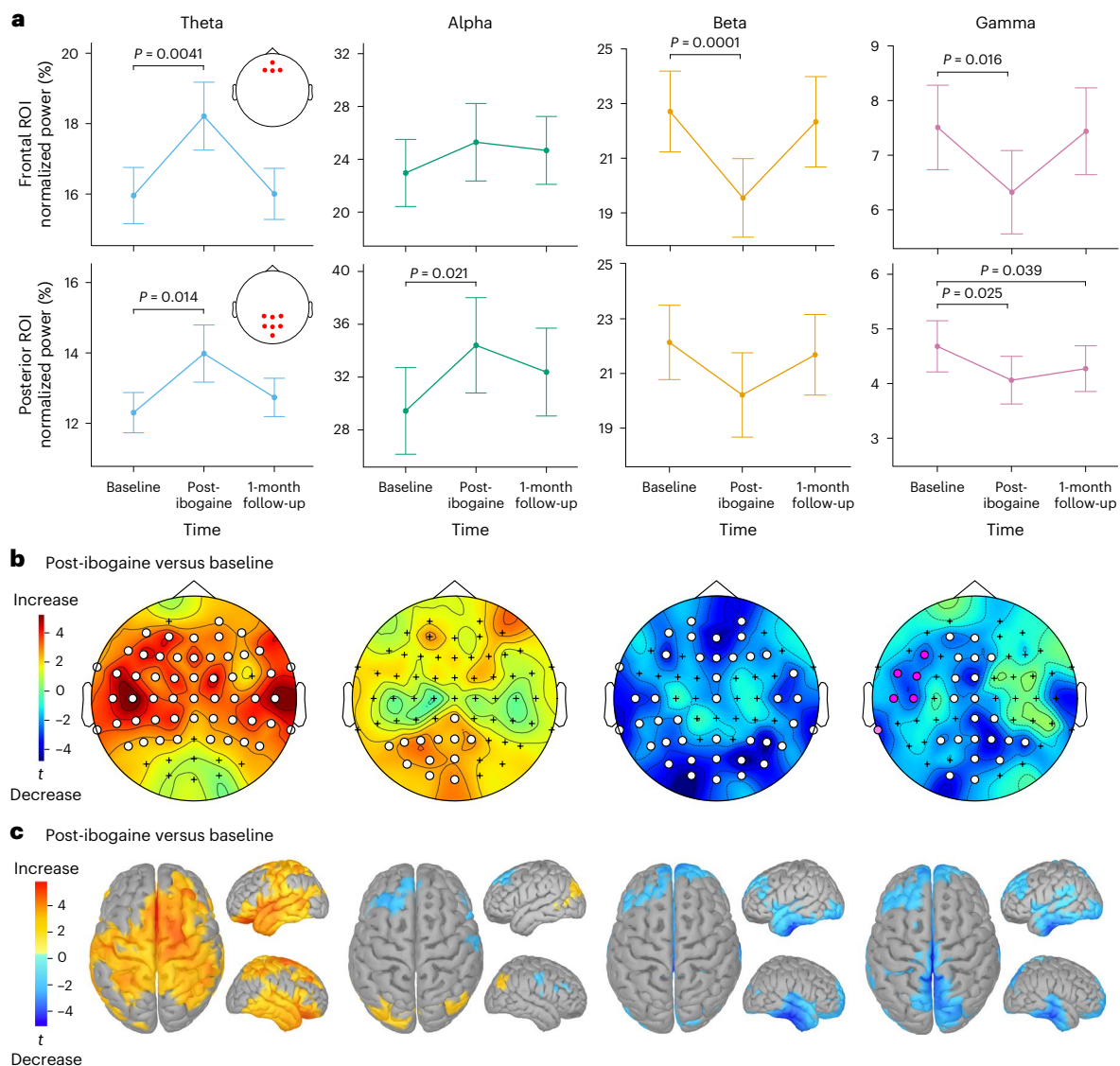


Fig. 2 | Enhancement of slower frequency activity and reduction of faster frequency activity after ibogaine treatment. a, In predefined frontal and posterior ROIs, theta ($n = 29$) and alpha (frontal $n = 30$; posterior $n = 29$) power increased post-ibogaine, and beta and gamma power ($n = 30$) decreased post-ibogaine, as compared with baseline (Dunnnett's test, two-sided). Reductions in posterior gamma power persisted at 1-month follow-up. Error bars represent the standard error of the mean. **b**, Channel-wide cluster-based permutation tests comparing normalized power post-ibogaine versus baseline at the sensor level

similarly revealed widespread increases in theta power, posterior increases in alpha power, and reductions in beta and gamma power. Significant clusters are displayed as white circles. A second significant cluster is displayed with pink circles for gamma power. **c**, Source estimation localized post-ibogaine increases in theta power to fronto-central and temporal regions, alpha power to parietal and occipital regions, and reductions in beta and gamma power to frontal and temporal regions. $t = t$ -statistic.

Oscillatory changes correlate with clinical outcomes

Significant correlations were observed between changes in theta/beta ratio and changes in cognitive inhibition after ibogaine treatment, as assessed using the Delis Kaplan Executive Function System (Color-Word Inhibition ('Stroop') Test)⁴¹. Specifically, increased theta/beta ratio post-ibogaine correlated with improved cognitive inhibition post-ibogaine in both frontal ($\rho = 0.54$, $P_{\text{FDR}} = 0.0026$) and posterior ($\rho = 0.59$, $P_{\text{FDR}} = 0.0015$) ROIs (Fig. 3b). This relationship was specific to cognitive inhibition, as changes in theta/beta ratio did not correlate significantly with changes in processing speed or sustained attention post-ibogaine. Changes in power, PAF, LZc and aperiodic components post-ibogaine did not correlate significantly with cognitive outcomes after FDR correction. Notably, however, increased posterior theta power and decreased posterior beta power post-ibogaine showed moderate correlations with improved

cognitive inhibition post-ibogaine, which were non-significant after FDR correction (theta: $\rho = 0.50$, $P_{\text{FDR}} = 0.052$, $P_{\text{uncorrected}} = 0.0052$; beta: $\rho = -0.45$, $P_{\text{FDR}} = 0.067$, $P_{\text{uncorrected}} = 0.013$).

Lowered posterior PAF post-ibogaine was significantly correlated with greater percentage improvement in PTSD symptoms at 1 month, as assessed using the clinician-administered PTSD scale (CAPS-5)⁴² ($\rho = 0.54$, $P_{\text{FDR}} = 0.011$; Fig. 4d). A similar relationship was observed between lowered posterior PAF post-ibogaine and 1-month percentage improvement in anxiety symptoms, as assessed using the Hamilton Anxiety Rating Scale (HAM-A⁴³; $\rho = 0.44$, $P_{\text{FDR}} = 0.058$); however, the correlation was non-significant after FDR correction. Given previous evidence of a relationship between PAF and arousal/alertness in particular^{14,44,45}, the relationship between lowered posterior PAF post-ibogaine and percentage improvement in the CAPS subscale for arousal and reactivity symptoms was also explored, and a similar

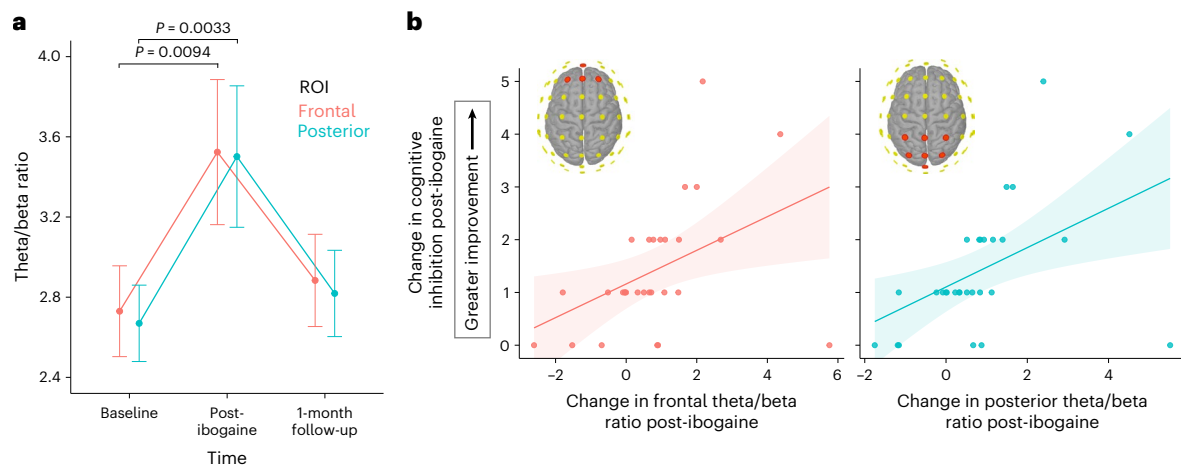


Fig. 3 | An increased ratio of slower to faster oscillations after ibogaine treatment, as indexed by theta/beta ratio, correlated with executive function improvements. a, In the frontal and posterior ROIs, theta/beta ratio increased significantly after ibogaine treatment ($n = 29$) compared with baseline, and these effects were not observed at 1-month follow-up ($n = 25$) (Dunnett's test, two-sided). Error bars represent the standard error of the mean. **b**, Scatterplots of the

relationship between increased theta/beta ratio post-ibogaine in each ROI and improved cognitive inhibition post-ibogaine ($n = 29$). For visualization purposes, the solid line represents a linear model fit, and the shaded areas represent the 95% confidence intervals. Cognitive inhibition was indexed using the Color-Word Inhibition scaled score. Red electrodes overlaid on the brain template represent the ROI for the respective theta/beta ratio.

relationship was observed ($\rho = 0.53$, $P = 0.0050$; Fig. 4d). A significant correlation was also observed between changes in the posterior ROI aperiodic exponent and percentage reduction in PTSD symptoms at 1 month ($\rho = 0.53$, $P_{\text{FDR}} = 0.015$). Changes in normalized power, theta/beta ratio, LZc and other aperiodic components post-ibogaine did not correlate significantly with 1-month psychiatric outcomes after FDR correction.

Pretreatment EEG markers of clinical outcomes

Greater improvement in cognitive inhibition post-ibogaine was significantly correlated with lower PAF pretreatment (global: $\rho = -0.54$, $P_{\text{FDR}} = 0.0045$; posterior: $\rho = -0.63$, $P_{\text{FDR}} = 0.0012$; Fig. 4c) and lower LZc pretreatment ($\rho = -0.51$, $P = 0.0038$; Fig. 5b). Baseline PAF and LZc were not significantly correlated with improved processing speed or sustained attention. In exploratory correlations between baseline measures, lower baseline PAF also correlated with lower baseline cognitive inhibition (see Extended Data Fig. 5 for details).

See Fig. 6 and Supplementary Fig. 3 for a summary of channel-wide relationships between baseline normalized power and improvement in CAPS-5 and HAM-A scores 1 month after ibogaine. After FDR correction, improvement in PTSD symptoms at 1-month follow-up correlated significantly with lower baseline alpha power and higher baseline delta and gamma power. Similarly, improvement in anxiety symptoms at 1-month follow-up correlated significantly with lower baseline alpha power and higher baseline beta and gamma power. Similar associations were observed in ROI-specific correlations (Supplementary Data 10). Channel-wide correlations with depressive symptom improvement at 1-month follow-up were non-significant after FDR correction (Supplementary Fig. 4).

Discussion

This study quantitatively investigated the effects of ibogaine on human cortical dynamics. Cortical oscillations and complexity were measured prospectively in SOVs with a history of TBI who suffered from marked disability, including PTSD, depression, anxiety and cognitive dysfunction, and who demonstrated striking improvements in these symptoms after ibogaine treatment⁵. We identified post-acute changes in cortical oscillations after ibogaine treatment across most EEG measures, including enhanced theta and alpha power, reduced beta and gamma power, increased theta/beta ratio, reduced global Lempel–Ziv complexity and

lowered PAF. PAF slowing was most prominent in the posterior cortex and sustained 1 month after treatment. Of note, when non-oscillatory components of the signal were removed, increases in theta and alpha power also persisted 1 month after treatment. Taken together, these findings suggest an overall slowing of spontaneous cortical oscillations and a shift to a more stable spatiotemporal pattern of cortical activity after ibogaine treatment. Changes in cortical oscillations showed moderate relationships with improved executive function and PTSD symptoms after treatment. In addition to being engaged by ibogaine treatment, baseline measures of cortical oscillations and neural complexity were associated with individual differences in executive function, PTSD and anxiety symptom improvements after MISTIC. Altogether, this study identified neurophysiological mechanisms and pretreatment EEG measures that relate to the therapeutic outcomes of treatment with ibogaine.

Post-acute drug effects of ibogaine

The observed transient changes in theta to gamma power and the complexity of spontaneous brain activity provide evidence of the post-acute drug effects of ibogaine. These initial effects of ibogaine on oscillations in theta, alpha, beta and gamma bands were localized to a range of frontal, parietal and temporal cortical regions, including substantial overlap with hubs of the default mode network. Effects localized to frontal and temporal cortices are particularly interesting to treating TBI neuropathology, since TBI has been found to affect primarily frontal and temporal gray matter, regardless of the site of impact⁴⁶. Interestingly, this shift toward theta and alpha power and reduction in spatiotemporal complexity after ibogaine treatment differs from many of the acute changes identified immediately after the administration of other psychedelic substances in healthy adults, such as broadband reductions in power^{26–31}, increases in delta power^{47,48} and increases in complexity^{31–33,49,50}. As such, the observed post-acute effects might be unique to the pharmacological mechanisms of ibogaine. The aperiodic slope of the power spectrum was also found to be post-acutely increased after ibogaine, potentially reflecting a shift in the excitation–inhibition balance in favor of inhibitory GABA synaptic currents^{40,51}. Importantly, these EEG measures of ibogaine's post-acute effects on neural function may be useful for personalizing ibogaine treatment; current ibogaine dosing techniques rely on subjective reports of ibogaine-induced symptoms rather than biological

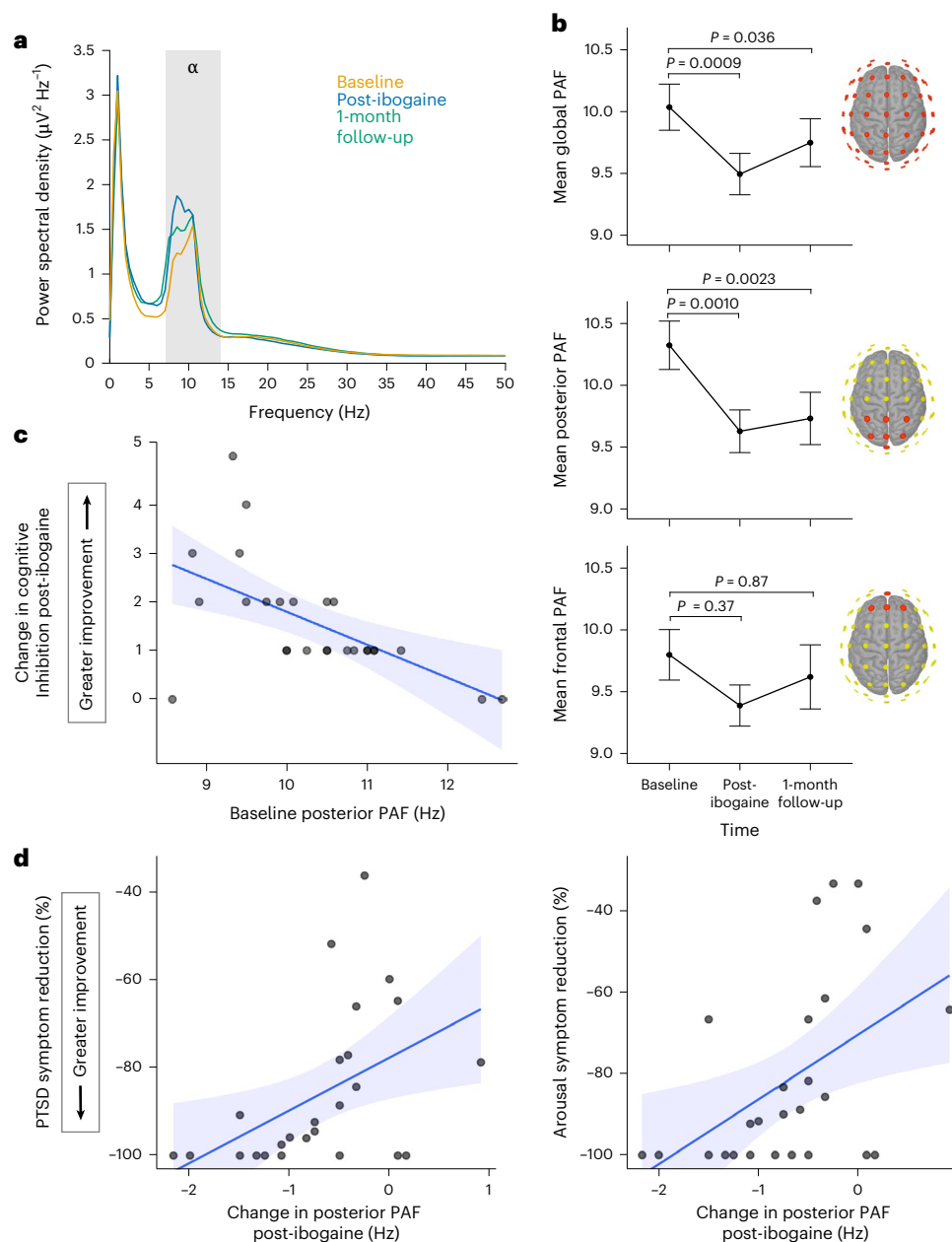


Fig. 4 | Ibogaine treatment lowers PAF, which was associated with psychiatric and cognitive outcomes. a, PAF was extracted from the power spectrum for each channel at each time point as the local maximum within the 7–14 Hz range. **b**, Global PAF was significantly lower post-ibogaine ($n = 26$), reflecting primarily a shift to a lower PAF in the posterior cortex, and this effect persisted 1 month after treatment ($n = 23$) (Dunnett's test, two-sided). Red electrodes overlayed on the brain template represent the ROI for the respective PAF calculation. Error bars

represent the standard error of the mean. **c**, Lower PAF before treatment showed a significant correlation with greater improvement in cognitive inhibition post-ibogaine ($n = 26$). **d**, Greater reductions in PAF post-ibogaine were significantly correlated with greater improvement in PTSD symptoms, and arousal in particular, at 1-month follow-up ($n = 25$). For visualization purposes, the blue line represents a linear model fit, and the shaded blue areas represent the 95% confidence intervals.

indicators of neural engagement. EEG measures of cortical oscillations are relatively low-cost to acquire and may therefore be useful as objective markers of optimal ibogaine dosing. For example, EEG monitoring is used to optimize the dosing of anesthetic drugs and can lead to lower rates of under- and over-dosing^{52,53}. Future studies on the real-time effects of ibogaine on cortical activity are needed to further explore these potential biomarkers of optimal ibogaine dosing.

The observed post-acute reduction in complexity 3.5 days after the administration of ibogaine may be in line with a neural annealing model of psychedelic treatments⁵⁴. According to this model, psychedelics may acutely increase entropy during administration, followed post-acutely by a return to a rebalanced, potentially lower entropy state. A similar

pattern has been described for meditation; for example, complexity increases acutely during the meditative state, but baseline complexity decreases with long-term meditation practice⁵⁵.

Neurophysiological correlates of ibogaine treatment outcomes

In addition, our findings offer insight into the neural mechanisms through which ibogaine may exert its therapeutic effects in TBI populations. Specifically, an increase in the relative dominance of theta rhythms (4–8 Hz) post-ibogaine, captured as an increased theta/beta ratio, showed a moderate relationship with improved executive function post-ibogaine. Of note, although potentially conflicting findings exist linking higher theta/beta ratios to worse cognitive

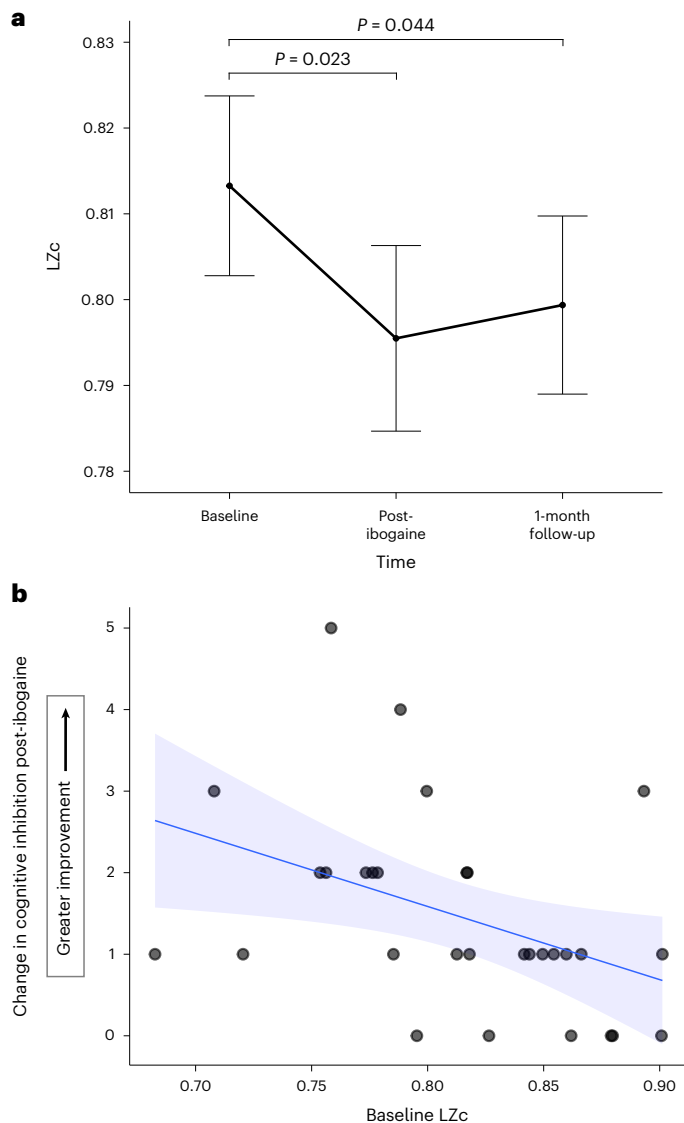


Fig. 5 | Ibogaine treatment reduces LZc. a, LZc was significantly lower post-ibogaine ($n = 30$), and this effect persisted at 1-month follow-up ($n = 27$) (Dunnett's test, two-sided). Error bars represent the standard error of the mean. After accounting for changes in spectral power, reductions in Lempel–Ziv complexity were specific to spatiotemporal complexity, rather than temporal complexity within electrodes (Supplementary Data 9), suggesting that ibogaine may primarily influence the diversity of neural activity patterns across electrodes. **b**, Lower LZc before treatment was significantly correlated with greater improvement in cognitive inhibition post-ibogaine ($n = 30$). For visualization purposes, the blue line represents a linear model fit, and the shaded blue area represents the 95% confidence interval.

control over emotional information⁵⁶, a similar relationship between higher theta/beta ratio at rest and greater inhibitory control has been observed previously in healthy adults³⁷, and increased frontal theta power has repeatedly been shown to be a mechanism for cognitive control^{58,59}. In addition, we report a specific relationship between post-acute within-subject changes in theta/beta ratio and changes in cognitive inhibition after treatment; therefore, this finding is distinct from previous cross-sectional studies examining theta/beta ratio as a between-subjects marker of cognitive control. A potentially related reduction in PAF⁶⁰ after treatment was also moderately associated with better PTSD outcomes. Future work should additionally assess whether these EEG changes relate to the real-time subjective intensity of the ibogaine experience.

It is possible that these changes in cortical oscillations associated with cognitive and psychiatric outcomes relate to the neuroplastic effects of ibogaine⁶¹. Nardou et al. recently showed in rodents that ibogaine can reopen critical learning periods in part through the induction of metaplasticity⁶². Although speculative, the neuroplastic effects of ibogaine may facilitate cognitive flexibility, thus enabling some of the observed therapeutic effects. In line with this idea, theta rhythms are associated with long-term potentiation⁶³, and our work suggests that ibogaine may promote theta rhythms and executive function concurrently. Accordingly, other types of interventions that are thought to promote both neuroplasticity and executive function, such as neuromodulation^{64–67} and meditation^{68–71}, have shown similar effects on cortical activity to those reported here, including enhanced theta power^{72–74} and decreased complexity⁵⁵. By contrast, advancing age is associated with reductions in metaplasticity, executive function and resting-state theta power^{75,76}, and higher theta power has been linked to better executive function in older adults^{76,77}. In addition, improvements in executive function have been shown to mediate the therapeutic effects of psychedelic substances, including ibogaine⁷⁸. Although further work is needed to identify causal relationships between ibogaine, theta oscillations, neuroplasticity and executive function, these lines of evidence suggest that the enhancement of theta oscillations after ibogaine treatment might reflect a transition into a more malleable brain state, which could allow some of the marked changes in mental state observed after ibogaine treatment.

Moreover, persisting reductions in PAF and neural complexity might relate to a reduction in hyperarousal after ibogaine treatment. TBI and PTSD have been linked to states of hyperarousal^{79,80}, which is associated with poorer executive function⁸¹. Elevated PAF has been observed in PTSD¹⁸, elevated Lempel–Ziv complexity has been observed in individuals with chronic stress⁸², and elevated PAF and complexity are both putative markers of higher arousal and alertness^{14,17,44,45,83}. Exploring this relationship, we found that PAF slowing post-ibogaine was associated with reduced arousal symptoms 1 month after treatment. The observed reductions of PAF and complexity that persisted 1 month after ibogaine treatment may therefore reflect a lasting reduction in hyperarousal at rest. There is evidence that reducing hyperarousal in treatment can mediate improvement in other PTSD symptom clusters⁸⁴.

Pretreatment EEG measures related to treatment outcomes

EEG measures of PAF, neural complexity and spectral power collected before treatment may also be valuable for predicting individual ibogaine treatment outcomes. In particular, lower baseline PAF and complexity were related to greater improvement in cognitive inhibition post-ibogaine. Accordingly, emerging evidence supports PAF as a biomarker for stratifying patients to different psychiatric interventions; for example, low baseline PAF has been shown to predict better response to specific types of antidepressant treatment⁸⁵. In addition, we found that the relative dominance of alpha versus delta, beta and gamma rhythms at baseline was related to improvement in PTSD and anxiety symptoms 1 month after ibogaine treatment. These results are similarly in line with a growing body of evidence showing that pretreatment EEG measures of spectral power can be used to predict psychiatric treatment outcomes^{38,86}. Further work is needed to assess the specificity of these potential biomarkers to ibogaine treatment to validate their potential use in the stratification of patients to different types of interventions.

Biological significance of changes in cortical oscillations

Findings of increased posterior alpha power and reduced delta power (Supplementary Data 2 and Extended Data Fig. 3) after ibogaine treatment might reflect the normalization of abnormally low alpha and high delta power previously reported after TBI^{7–11}. Accordingly, higher baseline delta power was associated with greater combat exposure (Extended Data Fig. 5). Increased theta power and theta/beta ratio, and

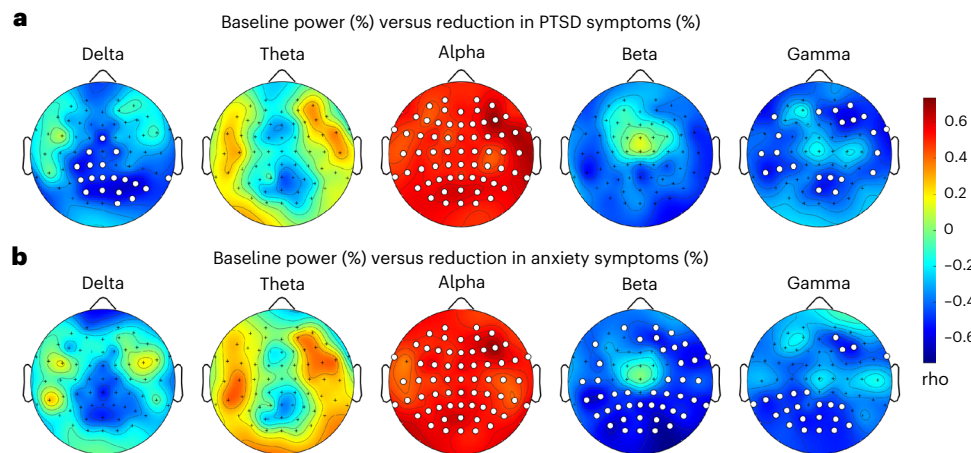


Fig. 6 | Pretreatment EEG measures of spectral power correlated with reduced PTSD and anxiety symptoms after ibogaine treatment. a, Topoplots showing channel-wide correlations between normalized baseline power and percentage reduction in CAPS scores at 1-month follow-up ($n = 29$). **b,** Topoplots showing

channel-wide correlations between normalized baseline power and percentage improvement in HAM-A scores at 1-month follow-up ($n = 29$). White electrodes signify statistical significance after FDR correction ($P_{\text{FDR}} < 0.05$).

lower PAF and complexity after ibogaine treatment, however, are not in line with the normalization of TBI-related neurophysiological impairments. These changes may instead index an alternative mechanism of the recovery process, such as neuroplasticity, or reflect the normalization of impairments related to specific symptom dimensions, such as hyperarousal. Future work with an age-matched healthy control comparison group is needed to clarify whether changes in neurophysiological measures after ibogaine reflect normalizing or compensatory changes in brain function.

Evidence from concurrent functional MRI–EEG suggests that the observed shift in the oscillatory profile post-ibogaine may also reflect changes in the activity of functional brain networks⁸⁷. For example, both increased resting-state theta power and reduced resting-state beta power have been correlated with less activity in regions of the default mode network^{88,89}. Source analysis revealed that enhanced theta power and reduced beta power after ibogaine were localized to several regions of the default mode network. Further investigation into the relationships between changes in spectral power and functional network activity and connectivity will help to clarify the full picture of cortical reorganization after ibogaine treatment.

Limitations

The findings reported here should be considered in the context of study limitations. First, this was a single-arm, open-label observational study, and future work including randomization to a control condition is needed to validate these initial findings and clarify the specificity of any effects of ibogaine administration. Expectation effects and other elements of the study intervention, such as coaching and the social context in which treatment was delivered, could have contributed to the current findings. However, the EEG effects were associated with the large psychiatric and cognitive benefits observed after treatment that are unlikely to have been driven exclusively by these other elements of the intervention. In addition, previous studies on the effects of placebo interventions on EEG spectral power have not consistently shown the changes in spectral measures reported here; for example, studies have reported no changes in power after placebo^{90–93}, increases in alpha power during placebo analgesia^{94,95}, and broadband (delta to beta) decreases in power after placebo in a psychedelics study³¹. Expanding on these previous studies, we also analyzed changes in power after placebo intervention in the EMBARC trial and did not identify significant changes in theta, beta or gamma power; however, left parietal alpha power was significantly increased after placebo (Supplementary Data 1 and Extended Data Fig. 2). The observed increases

in alpha power in particular after ibogaine may therefore be related to placebo effects. Second, the sample size was modest, with high homogeneity. As such, while our sample is largely representative of SOVs, future work in larger, more diverse populations, including other clinical populations, is needed to generalize these findings to other groups. Third, although the primary findings largely persisted when accounting for aperiodic activity, non-oscillatory components of the signal may have influenced post-acute beta and gamma power findings in particular. Last, correlations with clinical improvement were limited by the low variability in clinical responses; although associations with 1-month clinical outcomes were assessed instead of post-ibogaine clinical outcomes to mitigate this problem, the majority of participants still showed >80% improvement in Montgomery–Åsberg Depression Rating Scale (MADRS), CAPS and HAM-A scores at 1 month. Future work with more variability in treatment outcomes will help to clarify associations between cortical oscillations and clinical change.

Conclusions

In summary, as part of a prospective investigation of ibogaine treatment for veterans suffering from the sequelae of TBI, we identified both post-acute and persisting changes in neural complexity and the nature of cortical oscillations after ibogaine, which were related to psychiatric and cognitive treatment outcomes. By advancing our understanding of the neural mechanisms underlying this promising rapid treatment, our work identified several potential biomarkers of early drug effects and treatment response. With further investigation into the validity and replicability of these results, these biomarkers could enable (1) brain-based ibogaine dosing, (2) the optimization of treatment to engage specific therapeutic mechanisms and (3) the selection of optimal candidates for ibogaine treatment based on pretreatment neurophysiological profiles.

Methods

Participants

A total of 34 participants were screened, and 30 participants were eligible for the study and completed pre- and post-treatment assessments. All participants were male SOVs with a history of TBI resulting from blast exposure, head trauma or combat (mean \pm s.d. age = 44.9 ± 7.5). The mean \pm s.d. number of previous TBIs was 38.6 ± 52.4 , ranging in severity from mild ($n = 28$) to moderate ($n = 1$) and moderately severe ($n = 1$), as determined by the Ohio State University Screening for TBI exposure⁹⁶. The gender and racial/ethnic identity of participants were determined by self-report using provided classification terms.

Twenty-six of the participants identified as white, one as Hispanic, one as Native American and two as biracial (white and Native American). Diagnosed psychiatric disorders at entry into the study based on the Mini International Neuropsychiatric Interview included PTSD ($n = 23$), major depression ($n = 15$), anxiety disorder ($n = 14$) and alcohol use disorder ($n = 15$). In accordance with treatment protocols, participants discontinued medications with the potential to cause drug–drug interactions, including psychiatric medications and benzodiazepines⁵. Participants received compensation for completing study visits. Participant characteristics and study methods are described in further detail in Supplementary Table 1 and in previous work⁵.

Treatment

All participants were referred by the nonprofit Veterans Exploring Treatment Solutions, Inc. and independently scheduled for treatment with ibogaine at Ambio Life Sciences in Mexico. MISTIC treatment involved the co-administration of oral ibogaine (mean \pm s.d. total dose = 12.1 ± 1.2 mg kg⁻¹) with intravenous magnesium sulfate to protect against the cardiovascular effects of the drug, particularly Q–T interval prolongation^{5,97}. Participants were medically evaluated and received preparatory coaching about the ibogaine experience from a licensed therapist before treatment. Integration resources were also made available to participants after treatment. No psychotherapy was delivered during treatment. The effects of ibogaine can last 24–72 hours or longer⁹⁸; therefore, participants underwent continued monitoring for 72 hours after dosing. The MISTIC clinical trial was preregistered at ClinicalTrials.gov (NCT04313712).

Clinical and neuropsychological measures

Depressive symptoms were assessed using the clinician-administered MADRS⁹⁹, PTSD symptoms using the clinician-administered CAPS-5⁴², and anxiety symptoms using the HAM-A⁴³. A battery of neuropsychological tests was also performed at all study visits. In the current work, we focused on three neuropsychological measures that were substantially improved after ibogaine treatment⁵ and have previously been shown to relate to spectral power: (1) processing speed (Wechsler Adult Intelligence Scale—Fourth Edition, Processing Speed Index)¹⁰⁰, (2) cognitive inhibition (Delis Kaplan Executive Function System, Color–Word Inhibition)⁴¹ and (3) sustained attention (Conners' Continuous Performance Test—Third Edition)¹⁰¹. One participant was excluded from analyses of neurophysiological relationships with psychiatric outcomes as their baseline MADRS, CAPS and HAM-A scores were not consistent with the presence of psychiatric symptoms⁵. Six participants did not complete Conners' Continuous Performance Test—Third Edition (sustained attention) at baseline. REDCap electronic data capture tools hosted at Stanford University were used for data collection¹⁰².

EEG recording and preprocessing

See Fig. 1 for an overview of EEG procedures. Participants underwent resting-state EEG 2–3 days before ibogaine treatment ($n = 30$), 3.5 days post-ibogaine ($n = 30$) and 1 month post-ibogaine ($n = 27$). Three participants did not complete EEG recordings at the 1-month follow-up for logistical reasons. A total of 6 minutes of eyes-open EEG were recorded in two 3-minute segments with a short break in between recordings to promote wakefulness; this recording length has been shown previously to achieve high test–retest reliability^{103–106}. Recordings were performed with eyes open to further promote wakefulness and because eyes-open EEG spectral measures have previously been identified as robust predictors of psychiatric treatment outcomes³⁸. Participants were seated upright and instructed to fixate on centrally presented crosshairs, stay still and let their minds wander naturally without focusing on anything particular. Data were sampled at 10 kHz using 64 Ag–AgCl channels (actiCAP slim EEG cap; Brain Products GmbH) with an acti64CHamp Amplifier, and referenced to Cz during recording. Channels were

arranged according to the 10–10 system. Impedance was maintained at <10 k Ω in $>80\%$ of channels and <25 k Ω in $>99\%$ of channels.

EEG data preprocessing was performed offline using a combination of the EEGLAB toolbox¹⁰⁷ and ARTIST code in MATLAB, which is an automated EEG artifact rejection algorithm¹⁰⁸. The preprocessing pipeline consisted of the following steps. (1) Data were downsampled to 1 kHz. (2) A notch filter was applied for 60 Hz line noise and harmonics, and high-pass (1 Hz) and low-pass (50 Hz) filters were applied using windowed-sinc finite impulse response filters. (3) The beginning and end of each recording were trimmed to eliminate filter edge effects. (4) Bad-channel rejection was performed using a semi-automated method, including rejection based on impedance > 25 k Ω , detection of bridging, or persistent noise identified automatically¹⁰⁸ then visually inspected by an experienced rater ($< 15\%$ of channels were rejected). For four recordings, an impedance threshold of 50 k Ω was applied to maintain the channel rejection limit; however, visual inspection of the data indicated good-quality signal in all remaining channels. Sensitivity analyses were performed, excluding recordings in which $>10\%$ of channels showed impedance > 25 k Ω (Supplementary Data 4). Spherical interpolation of missing channels was performed. (5) Data were binned into 2-second epochs, and epochs containing excessive noise were discarded (mean \pm s.d. epochs rejected = $6.1 \pm 2.6\%$; range 1.7–13.9%). (6) Data were re-referenced to the average. (7) Independent component analysis was performed using the Infomax algorithm¹⁰⁹ with principal component analysis dimension reduction (determined as the fewest principal components that explain $>99.9\%$ of the variance¹⁰⁸; average principal components: 50.2 ± 4.7 ; range 35–59), and components reflecting ocular and muscle artifacts were removed. (8) Data were re-referenced to the average. All steps were performed by an experienced rater who was blind to the visit number and clinical scores associated with each recording.

MRI

A T1-weighted anatomical MRI scan was also performed for coregistration with EEG. MRI scans were performed using a 3T MRI scanner equipped with a 32-channel head coil (GE Discovery MR750). A T1-weighted anatomical MRI scan was acquired using the GE BRAVO sequence (TR = 6.39 ms; TE = 2.62 ms; flip angle = 12° ; voxel size = $0.9 \times 0.9 \times 0.9$ mm). Two participants did not undergo an MRI due to the presence of metal fragments in the eyes.

Spectral measures

To reduce the dimensionality of the data in our primary analyses, two ROIs were defined a priori: a medial frontal ROI (AFz, F1, Fz, F2) and a medial posterior ROI (CP1, CPz, CP2, P1, Pz, P2, POz) approximating sensor-space ROIs previously found to show acute changes in oscillatory power after the administration of classic psychedelics²⁹. Power spectral density ($\mu\text{V}^2 \text{Hz}^{-1}$) was calculated for all channels using Welch's method with 2-second Hamming windows and 50% overlap. Mean broadband power (1–50 Hz) for each epoch was z scored with respect to all epochs, and outlier epochs were excluded ($z > 1.96$; $<7\%$ of epochs rejected). The average final recording length was 336 s (range: 310–356 s). The total percentage of epochs rejected did not differ significantly between study time points (baseline versus post-ibogaine: $t_{29} = 0.11$, $P = 0.92$; baseline versus 1-month follow-up: $t_{26} = 0.78$, $P = 0.44$). Power was calculated in predefined canonical frequency bands related to different neurophysiological mechanisms: delta (1–4 Hz), theta (4–8 Hz), alpha (8–13 Hz), beta (13–30 Hz) and gamma (30–50 Hz). Power values were normalized to broadband power by dividing the Riemann sum of power within a predefined band by the Riemann sum of power across all frequencies (1–50 Hz), using the following equation:

$$\text{Normalized power}_{a-b\text{Hz}} = \frac{\sum_a^b P(f) \times \Delta x(f)}{\sum_1^{50} P(f) \times \Delta x(f)} \times 100\%$$

where a and b indicate the lower and upper bounds of the frequency range of interest, $P(f)$ represents absolute power at frequency f ($\text{mcV}^2 \text{ Hz}^{-1}$), and Δx represents the frequency bin width (Hz). Normalized power for each band therefore reflects that band's percentage of total power. Theta/beta ratio was computed as the ratio of absolute theta power over absolute beta power. For each ROI, normalized power and theta/beta ratio were averaged across ROI channels.

PAF was calculated for each channel using custom MATLAB scripts that identified the frequency with local maximum power within the 7–14 Hz frequency range^{68,110,111}. All spectra were reviewed to verify the accuracy of PAF estimates. PAF was estimated globally by averaging across all channels, and the regional specificity of any PAF effects was explored by averaging channels within each predefined ROI. Channels in which no peak could be identified were excluded from the PAF estimate, and participants were excluded if no peak was identified in >20% of channels ($n = 4$ excluded; in accordance with previous reports that 10–15% of individuals do not show a dominant alpha rhythm¹¹²).

In exploratory analyses of changes in the non-oscillatory background spectral decay using the FOOOF algorithm⁴⁰, the ROI aperiodic exponent and offset were computed using the following parameters: frequency range = 1–50 Hz; peak width = 1–12 Hz; max peaks = infinite; peak threshold = 2 s.d.; aperiodic mode = fixed. The potential influence of the aperiodic components on the primary results was explored by subtracting the aperiodic component from the power spectrum and recomputing normalized power using the flattened spectrum.

Source localization was performed using the Brainstorm toolbox¹¹³ to identify where changes in spectral power at the sensor level were localized in brain space. Source localization to the cortical surface was performed using minimum norm estimates and a boundary element model of the head using individual T1 images, or the ICBM152 standard MRI brain template when no individual MRI was available ($n = 2$; see Supplementary Fig. 2 for sensitivity analyses excluding these two participants). Unconstrained dipole orientations¹¹⁴ were generated at 15,000 cortical vertices. Inverse modeling was performed using L2-minimum norm estimation with depth weighting, and using the diagonal noise covariance. After transformation into source space, power spectral density was computed using the Welch method. Power was extracted for predefined frequency bands, normalized to total power (1–50 Hz) and projected onto the cortical surface of a template brain for group analysis. Regions showing a significant change in power were identified using Desikan–Killiany and Schaeffer 100-parcel 7-network atlases (Supplementary Table 2).

Considering the lack of a placebo control group in the current study, the publicly available EMBARC dataset was used to explore potential placebo effects on resting-state EEG measures of spectral power¹¹⁵. In an age-matched subset of participants with depression ($n = 30$), a total of 4 minutes of resting-state EEG data were collected before and after 1 week of placebo intervention. Source-space changes in spectral power were compared between baseline and 1-week time points using permutation tests (5,000 permutations, $P < 0.05$ threshold). See Supplementary Data 1 for further details.

Lempel–Ziv complexity

Lempel–Ziv complexity quantifies the number of unique patterns in the EEG signal, which reflects the diversity of activity patterns in both time and space. The Lempel–Ziv–Welch algorithm¹¹⁶ was applied to 2-second epochs at a 1 kHz sampling rate. Lempel–Ziv complexity was also computed using 10-second epochs to verify that the results were not sensitive to epoch length (Supplementary Data 9). A 30 Hz low-pass filter was applied to the data to ensure that complexity measures were not impacted by muscle activity. Complexity was computed on the mean binarized envelope of the signal, which was obtained via Hilbert Transform. Greater Lempel–Ziv complexity values reflect a larger number of non-redundant sub-sequences in the data, and therefore more randomness in the signal.

Two variants of Lempel–Ziv complexity were computed, in line with previous studies^{33,116}: LZc captures complexity within and across channels, thus capturing both temporal and spatial signal diversity, whereas LZs captures the complexity of each channel separately, later averaged, thus capturing only temporal signal diversity. LZc and LZs were normalized to the number of patterns in the temporally shuffled binarized signal (range 0–1, where 1 = maximum diversity). As an additional control to account for changes in the spectral profile of the data, raw values were also normalized using a phase-shuffled signal. Surrogate data were generated by phase randomization^{117,118}, where phase values obtained by Fourier transform are randomized then projected back into the time domain via inverse Fourier transform, which retains the spectral properties of the original signal while increasing overall diversity. For phase-randomized normalization, the raw LZc or LZs value was divided by the number of patterns in the phase-shuffled signal.

Statistics

Primary analyses consisted of linear mixed-effects models testing for the effect of time on spectral measures in predefined ROIs. Linear mixed-effects models included time point as a categorical fixed effect (baseline, post-treatment and 1-month follow-up) and participant as a random effect. Age, combat exposure and number of TBIs were included as covariates, given previous evidence that these factors might influence spectral power^{76,119,120}. For 3 participants, the number of TBIs was too high to estimate (for example, several hundred lifetime TBIs); therefore, these values were imputed as 5 s.d. above the mean. The distributions of model residuals were checked using histograms and quantile–quantile plots. Skew present due to outliers was addressed by excluding band-specific power outliers from each ROI (z score > 3; 1.4% of observations removed; see Supplementary Data 4 for sensitivity analyses including these outliers). All models were corrected for multiple comparisons using FDR correction (accounting for all frequency bands and ROIs). Post hoc comparisons of spectral power at baseline versus post-treatment and 1-month follow-up were performed using Dunnett's test to account for multiple comparisons¹²¹. Correlations with predefined psychiatric and cognitive outcomes were calculated using FDR-corrected Spearman's rho. The primary aims were preregistered at [osf.io](https://osf.io/24trc/) (<https://osf.io/24trc/>).

Controlling for the Type 1 error rate, cluster-based permutation tests were performed in sensor space using 5,000 permutations and a cluster-forming threshold of $P < 0.05$ (two-tailed)¹²². Similarly, permutation tests using 5,000 permutations and a $P < 0.05$ threshold were performed to identify where significant changes in spectral power occurred in source space. Cluster-based permutation tests were similarly performed exploring pre- to post-treatment changes in power across all frequencies (1–50 Hz) and 64 channels.

Inclusion and ethics

All research procedures were approved by the Stanford University Institutional Review Board (54095). We complied with all relevant ethical regulations. Written informed consent was obtained from all participants. Roles and responsibilities were agreed on among authors and collaborators. This investigation was preregistered at [osf.io](https://osf.io/24trc/) (<https://osf.io/24trc/>).

Reporting summary

Further information on research design is available in the Nature Portfolio Reporting Summary linked to this article.

Data availability

Owing to the sensitivity of psychiatric patient data, our IRB requires individualized review before data sharing. We have produced anonymized data related to the present findings for sharing with all scientists with research and data safeguarding plans that comport

with Stanford University guidelines. Anonymized data sharing does not require the use of a data use agreement. Please contact the corresponding author with data-sharing requests with an approximate response time within 90 days. Data from EMBARC are publicly available and can be accessed on request via https://nda.nih.gov/edit_collection.html?id=2199.

Code availability

The Matlab EEGLAB toolbox used for preprocessing and sensor-space spectral measures can be downloaded from <https://sccn.ucsd.edu/eeqlab/download.php>. ROI-based statistical analyses were performed using R version 4.3.1 (in RStudio v.2023.06.0) publicly available packages readxl v.1.4.2, lmerTest v.3.1-3, emmeans v.1.8.7 and rstatix v.0.7.2. Cluster-based permutation tests were performed using the freely available python MNE toolbox (mne.stats.permutation_cluster_test). Source estimation was performed using MATLAB Brainstorm, which is freely available (<https://neuroimage.usc.edu/bst/download.php>). Lempel–Ziv complexity measures were computed using publicly available code from Schartner et al. 2015 (ref. 116) (<https://doi.org/10.1371/journal.pone.0133532.s002>) and the SIFT EEGLAB plugin (https://github.com/sccn/SIFT/blob/master/stat/stat_surrogateGen.m). The FOOOF toolbox v1.1 for calculating aperiodic components of the EEG signal is publicly available (<https://fooof-tools.github.io/fooof/>). Other scripts used to analyze the data of this study are available at https://github.com/achaiken/lbogaine_rsEEG_project.

References

- Draper, K. & Ponsford, J. Cognitive functioning ten years following traumatic brain injury and rehabilitation. *Neuropsychology*. **22**, 618–625 (2008).
- Bryant, R. A. et al. The psychiatric sequelae of traumatic injury. *Am. J. Psychiatry* **167**, 312–320 (2010).
- Steenkamp, M. M., Litz, B. T. & Marmar, C. R. First-line psychotherapies for military-related PTSD. *JAMA* **323**, 656–657 (2020).
- Alexander, W. Pharmacotherapy for post-traumatic stress disorder in combat veterans. *Pharm. Ther.* **37**, 32–38 (2012).
- Cherian, K. N. et al. Magnesium–ibogaine therapy in veterans with traumatic brain injuries. *Nat. Med.* <https://doi.org/10.1038/s41591-023-02705-w> (2024).
- Davis, A. K., Averill, L. A., Sepeda, N. D., Barsuglia, J. P. & Amoroso, T. Psychedelic treatment for trauma-related psychological and cognitive impairment among US special operations forces veterans. *Chronic Stress* **4**, 247054702093956 (2020).
- Modarres, M. H., Kuzma, N. N., Kretzmer, T., Pack, A. I. & Lim, M. M. EEG slow waves in traumatic brain injury: convergent findings in mouse and man. *Neurobiol. Sleep Circadian Rhythms* **2**, 59–70 (2017).
- Haneef, Z., Levin, H. S., Frost, J. D. & Mizrahi, E. M. Electroencephalography and quantitative electroencephalography in mild traumatic brain injury. *J. Neurotrauma* **30**, 653–656 (2013).
- Buchanan, D. M., Ros, T. & Nahas, R. Elevated and slowed EEG oscillations in patients with post-concussive syndrome and chronic pain following a motor vehicle collision. *Brain Sci.* **11**, 537 (2021).
- Lewine, J. D. et al. Quantitative EEG biomarkers for mild traumatic brain injury. *J. Clin. Neurophysiol.* **36**, 298–305 (2019).
- Franke, L. M., Walker, W. C., Hoke, K. W. & Wares, J. R. Distinction in EEG slow oscillations between chronic mild traumatic brain injury and PTSD. *Int. J. Psychophysiol.* **106**, 21–29 (2016).
- Luo, Q. et al. Complexity analysis of resting state magnetoencephalography activity in traumatic brain injury patients. *J. Neurotrauma* **30**, 1702–1709 (2013).
- Coull, J. T. Neural correlates of attention and arousal: insights from electrophysiology, functional neuroimaging and psychopharmacology. *Prog. Neurobiol.* **55**, 343–361 (1998).
- Braboszcz, C. & Delorme, A. Lost in thoughts: neural markers of low alertness during mind wandering. *Neuroimage*. **54**, 3040–3047 (2011).
- Makeig, S. & Inlow, M. Lapse in alertness: coherence of fluctuations in performance and EEG spectrum. *Electroencephalogr. Clin. Neurophysiol.* **86**, 23–35 (1993).
- Lim, C. L. et al. The relationship between quantified EEG and skin conductance level. *Int. J. Psychophysiol.* **21**, 151–162 (1996).
- Zhang, X. S., Roy, R. J. & Jensen, E. W. EEG complexity as a measure of depth of anesthesia for patients. *IEEE Trans. Biomed. Eng.* **48**, 1424–1433 (2001).
- Wahbeh, H. & Oken, B. S. Peak high-frequency HRV and peak alpha frequency higher in PTSD. *Appl. Psychophysiol. Biofeedback* **38**, 57–69 (2013).
- Eidelman-Rothman, M., Levy, J. & Feldman, R. Alpha oscillations and their impairment in affective and post-traumatic stress disorders. *Neurosci. Biobehav. Rev.* **68**, 794–815 (2016).
- Olbrich, S., Van Dinteren, R. & Arns, M. Personalized medicine: review and perspectives of promising baseline EEG biomarkers in major depressive disorder and attention deficit hyperactivity disorder. *Neuropsychobiology* **72**, 229–240 (2015).
- Lau, Z. J., Pham, T., Chen, S. H. A. & Makowski, D. Brain entropy, fractal dimensions and predictability: a review of complexity measures for EEG in healthy and neuropsychiatric populations. *Eur. J. Neurosci.* **56**, 5047–5069 (2022).
- González-Trujano, M. E. et al. *Tabernaemontana arborea* and ibogaine induce paroxysmal EEG activity in freely moving mice: involvement of serotonin 5-HT 1A receptors. *Neurotoxicology* **89**, 79–91 (2022).
- González, J. et al. EEG gamma band alterations and REM-like traits underpin the acute effect of the atypical psychedelic ibogaine in the rat. *ACS Pharmacol. Transl. Sci.* **4**, 517–525 (2021).
- Binienda, Z. et al. Alteration in electroencephalogram and monoamine concentrations in rat brain following ibogaine treatment. *Ann. N. Y. Acad. Sci.* **844**, 265–273 (1998).
- Carhart-Harris, R. et al. Trial of psilocybin versus escitalopram for depression. *N. Engl. J. Med.* **384**, 1402–1411 (2021).
- Kometer, M., Pokorny, T., Seifritz, E. & Volleinweider, F. X. Psilocybin-induced spiritual experiences and insightfulness are associated with synchronization of neuronal oscillations. *Psychopharmacology* **232**, 3663–3676 (2015).
- Muthukumaraswamy, S. D. et al. Broadband cortical desynchronization underlies the human psychedelic state. *J. Neurosci.* **33**, 15171–15183 (2013).
- Carhart-Harris, R. L. et al. Neural correlates of the LSD experience revealed by multimodal neuroimaging. *Proc. Natl Acad. Sci. USA* **113**, 4853–4858 (2016).
- Murray, C. H. et al. Low doses of LSD reduce broadband oscillatory power and modulate event-related potentials in healthy adults. *Psychopharmacology* **239**, 1735–1747 (2022).
- Riba, J., Anderer, P., Jané, F., Saletu, B. & Barbanoj, M. J. Effects of the South American psychoactive beverage ayahuasca on regional brain electrical activity in humans: a functional neuroimaging study using low-resolution electromagnetic tomography. *Neuropsychobiology* **50**, 89–101 (2004).
- Timmermann, C. et al. Neural correlates of the DMT experience assessed with multivariate EEG. *Sci. Rep.* **9**, 16324 (2019).
- Timmermann, C. et al. Human brain effects of DMT assessed via EEG-fMRI. *Proc. Natl Acad. Sci. USA* **120**, e2218949120 (2023).
- Schartner, M. M., Carhart-Harris, R. L., Barrett, A. B., Seth, A. K. & Muthukumaraswamy, S. D. Increased spontaneous MEG signal diversity for psychoactive doses of ketamine, LSD and psilocybin. *Sci. Rep.* **7**, 46421 (2017).

34. Brown, T. K., Noller, G. E. & Denenberg, J. O. Ibogaine and subjective experience: transformative states and psychopharmacotherapy in the treatment of opioid use disorder. *J. Psychoactive Drugs*. **51**, 155–165 (2019).
35. Schenberg, E. E. et al. A phenomenological analysis of the subjective experience elicited by ibogaine in the context of a drug dependence treatment. *J. Psychedelic Stud.* **1**, 74–83 (2017).
36. Wasko, M. J., Witt-Enderby, P. A. & Surratt, C. K. DARK classics in chemical neuroscience: ibogaine. *ACS Chem. Neurosci.* **9**, 2475–2483 (2018).
37. Litjens, R. P. W. & Brunt, T. M. How toxic is ibogaine? *Clin. Toxicol.* **54**, 297–302 (2016).
38. Wu, W. et al. An electroencephalographic signature predicts antidepressant response in major depression. *Nat. Biotechnol.* **38**, 439–447 (2020).
39. Angelidis, A., Van Der Does, W., Schakel, L. & Putman, P. Frontal EEG theta/beta ratio as an electrophysiological marker for attentional control and its test-retest reliability. *Biol. Psychol.* **121**, 49–52 (2016).
40. Donoghue, T. et al. Parameterizing neural power spectra into periodic and aperiodic components. *Nat. Neurosci.* **23**, 1655–1665 (2020).
41. Delis, D. C., Kaplan, E. & Kramer, J. H. *Delis-Kaplan Executive Function System (D-KEFS)* (APAPsycTests, 2001); <https://doi.org/10.1037/t15082-000>
42. Weathers, F. W. et al. The Clinician-Administered PTSD Scale for DSM-5 (CAPS-5): development and initial psychometric evaluation in military veterans. *Psychol. Assess.* **30**, 383–395 (2018).
43. Hamilton, M. The assessment of anxiety states by rating. *Br. J. Med. Psychol.* **32**, 50–55 (1959).
44. Jann, K., Koenig, T., Dierks, T., Boesch, C. & Federspiel, A. Association of individual resting state EEG alpha frequency and cerebral blood flow. *Neuroimage*. **51**, 365–372 (2010).
45. Gutmann, B. et al. Effects of physical exercise on individual resting state EEG alpha peak frequency. *Neural Plast.* **2015**, 717312 (2015).
46. Ommaya, A. K. Head injury mechanisms and the concept of preventive management: a review and critical synthesis. *J. Neurotrauma* **12**, 527–546 (1995).
47. Frohlich, J., Mediano, P. A. M., Bavato, F. & Gharabaghi, A. Paradoxical pharmacological dissociations result from drugs that enhance delta oscillations but preserve consciousness. *Commun. Biol.* **6**, 654 (2023).
48. Blackburne, G. et al. Complex slow waves radically reorganise human brain dynamics under 5-MeO-DMT. Preprint at *BioRxiv* <https://doi.org/10.1101/2024.10.04.616717> (2024).
49. Viol, A., Palhano-Fontes, F., Onias, H., De Araujo, D. B. & Viswanathan, G. M. Shannon entropy of brain functional complex networks under the influence of the psychedelic ayahuasca. *Sci. Rep.* **7**, 7388 (2017).
50. Siegel, J. S. et al. Psilocybin desynchronizes the human brain. *Nature* **632**, 131–138 (2024).
51. Gao, R., Peterson, E. J. & Voytek, B. Inferring synaptic excitation/inhibition balance from field potentials. *Neuroimage*. **158**, 70–78 (2017).
52. Chan, M. T. V. et al. American Society for Enhanced Recovery and Perioperative Quality Initiative Joint Consensus Statement on the Role of Neuromonitoring in Perioperative Outcomes: Electroencephalography. *Anesth. Analg.* **130**, 1278–1291 (2020).
53. Punjasawadwong, Y., Phongchiewboon, A. & Bunchungmongkol, N. Bispectral index for improving anaesthetic delivery and postoperative recovery. *Cochrane Library* <https://doi.org/10.1002/14651858.CD003843.pub3> (2014).
54. Carhart-Harris, R. L. et al. Canalization and plasticity in psychopathology. *Neuropharmacology* **226**, 109398 (2023).
55. Atad, D. A., Mediano, P. A., Rosas, F. E. & Berkovich-Ohana, A. Meditation and complexity: a review and synthesis of evidence. *Neurosci. Conscious.* **2025**, niaf013 (2025).
56. Angelidis, A., Hagenaaars, M., Van Son, D., Van Der Does, W. & Putman, P. Do not look away! Spontaneous frontal EEG theta/beta ratio as a marker for cognitive control over attention to mild and high threat. *Biol. Psychol.* **135**, 8–17 (2018).
57. Lansbergen, M. M., Schutter, D. J. L. G. & Kenemans, J. L. Subjective impulsivity and baseline EEG in relation to stopping performance. *Brain Res.* **1148**, 161–169 (2007).
58. Cavanagh, J. F. & Frank, M. J. Frontal theta as a mechanism for cognitive control. *Trends Cogn. Sci.* **18**, 414–421 (2014).
59. Zavala, B. et al. Cognitive control involves theta power within trials and beta power across trials in the prefrontal-subthalamic network. *Brain* **141**, 3361–3376 (2018).
60. Lansbergen, M. M., Arns, M., Van Dongen-Boomsma, M., Spronk, D. & Buitelaar, J. K. The increase in theta/beta ratio on resting-state EEG in boys with attention-deficit/hyperactivity disorder is mediated by slow alpha peak frequency. *Prog. Neuropsychopharmacol. Biol. Psychiatry* **35**, 47–52 (2011).
61. Ly, C. et al. Psychedelics promote structural and functional neural plasticity. *Cell Rep.* **23**, 3170–3182 (2018).
62. Nardou, R. et al. Psychedelics reopen the social reward learning critical period. *Nature* **618**, 790–798 (2023).
63. Larson, J., Wong, D. & Lynch, G. Patterned stimulation at the theta frequency is optimal for the induction of hippocampal long-term potentiation. *Brain Res.* **368**, 347–350 (1986).
64. Ilieva, I. P. et al. Age-related repetitive transcranial magnetic stimulation effects on executive function in depression: a systematic review. *Am. J. Geriatr. Psychiatry*. **26**, 334–346 (2018).
65. Semkovska, M. & McLoughlin, D. M. Objective cognitive performance associated with electroconvulsive therapy for depression: a systematic review and meta-analysis. *Biol. Psychiatry* **68**, 568–577 (2010).
66. Fitzsimmons, S. M. D. D., Oostra, E., Postma, T. S., Van Der Werf, Y. D. & Van Den Heuvel, O. A. Repetitive transcranial magnetic stimulation-induced neuroplasticity and the treatment of psychiatric disorders: state of the evidence and future opportunities. *Biol. Psychiatry* <https://doi.org/10.1016/j.biopsych.2023.11.016> (2023).
67. Dukart, J. et al. Electroconvulsive therapy-induced brain plasticity determines therapeutic outcome in mood disorders. *Proc. Natl Acad. Sci. USA* **111**, 1156–1161 (2014).
68. Sagar, M. et al. Intensive training induces longitudinal changes in meditation state-related EEG oscillatory activity. *Front Hum Neurosci.* <https://doi.org/10.3389/fnhum.2012.00256> (2012).
69. Sleimen-Malkoun, R., Devillers-Réolon, L. & Temprado, J. J. A single session of mindfulness meditation may acutely enhance cognitive performance regardless of meditation experience. *PLoS ONE* <https://doi.org/10.1371/journal.pone.0282188> (2023).
70. Davidson, R. J. & McEwen, B. S. Social influences on neuroplasticity: stress and interventions to promote well-being. *Nat. Neurosci.* **15**, 689–695 (2012).
71. You, T. & Ogawa, E. F. Effects of meditation and mind-body exercise on brain-derived neurotrophic factor: a literature review of human experimental studies. *Sports Med. Health Sci.* **2**, 7–9 (2020).
72. Lomas, T., Iltzan, I. & Fu, C. H. Y. A systematic review of the neurophysiology of mindfulness on EEG oscillations. *Neurosci. Biobehav. Rev.* **57**, 401–410 (2015).
73. Noh, N. A., Fuggetta, G., Manganotti, P. & Fiaschi, A. Long lasting modulation of cortical oscillations after continuous theta burst transcranial magnetic stimulation. *PLoS ONE* **7**, e35080–12 (2012).
74. Hill, A. T. et al. Modulation of functional network properties in major depressive disorder following electroconvulsive therapy (ECT): a resting-state EEG analysis. *Sci. Rep.* **10**, 17057 (2020).

75. Lissemore, J. I., Wengle, L., Daskalakis, Z. J. & Blumberger, D. M. Insights into aging using transcranial magnetic stimulation. In *Factors Affecting Neurological Aging* (eds Martin, C. et al.) 337–348 (Elsevier, 2021); <https://doi.org/10.1016/B978-0-12-817990-1.00030-5>
76. Vlahou, E. L., Thurm, F., Kolassa, I. T. & Schlee, W. Resting-state slow wave power, healthy aging and cognitive performance. *Sci. Rep.* **4**, 5101 (2014).
77. Finnigan, S. & Robertson, I. H. Resting EEG theta power correlates with cognitive performance in healthy older adults. *Psychophysiology* **48**, 1083–1087 (2011).
78. Davis, A. K., Barrett, F. S. & Griffiths, R. R. Psychological flexibility mediates the relations between acute psychedelic effects and subjective decreases in depression and anxiety. *J. Context. Behav. Sci.* **15**, 39–45 (2020).
79. Frewen, P. A. & Lanius, R. A. Toward a psychobiology of posttraumatic self-dysregulation: reexperiencing, hyperarousal, dissociation, and emotional numbing. *Ann. N. Y. Acad. Sci.* **1071**, 110–124 (2006).
80. Porter, K. E. et al. Postconcussive symptoms (PCS) following combat-related traumatic brain injury (TBI) in veterans with posttraumatic stress disorder (PTSD): Influence of TBI, PTSD, and depression on symptoms measured by the Neurobehavioral Symptom Inventory (NSI). *J. Psychiatr. Res.* **102**, 8–13 (2018).
81. Jurick, S. M. et al. Independent and synergistic associations between TBI characteristics and PTSD symptom clusters on cognitive performance and postconcussive symptoms in Iraq and Afghanistan veterans. *J. Neuropsychiatry Clin. Neurosci.* **33**, 98–108 (2021).
82. Peng, H. et al. A method of identifying chronic stress by EEG. *Pers. Ubiquitous Comput.* **17**, 1341–1347 (2013).
83. Andriillon, T., Poulsen, A. T., Hansen, L. K., Léger, D. & Kouider, S. Neural markers of responsiveness to the environment in human sleep. *J. Neurosci.* **36**, 6583–6596 (2016).
84. Crawford, J. N., Talkovsky, A. M., Bormann, J. E. & Lang, A. J. Targeting hyperarousal: Mantram Repetition Program for PTSD in US veterans. *Eur. J. Psychotraumatol.* **10**, 1665768 (2019).
85. Voetterl, H. T. S. et al. Alpha peak frequency-based Brainmarker-I as a method to stratify to pharmacotherapy and brain stimulation treatments in depression. *Nat. Ment. Health.* **1**, 1023–1032 (2023).
86. Kim, S., Yang, C., Dong, S. Y. & Lee, S. H. Predictions of tDCS treatment response in PTSD patients using EEG based classification. *Front Psychiatry* **13**, 876036 (2022).
87. Mantini, D., Perrucci, M. G., Del Gratta, C., Romani, G. L. & Corbetta, M. Electrophysiological signatures of resting state networks in the human brain. *Proc. Natl Acad. Sci. USA* **104**, 13170–13175 (2007).
88. Scheeringa, R. et al. Frontal theta EEG activity correlates negatively with the default mode network in resting state. *Int. J. Psychophysiol.* **67**, 242–251 (2008).
89. Laufs, H. et al. Electroencephalographic signatures of attentional and cognitive default modes in spontaneous brain activity fluctuations at rest. *Proc. Natl. Acad. Sci. USA* **100**, 11053–11058 (2003).
90. Leuchter, A. F., Cook, I. A., Witte, E. A., Morgan, M. & Abrams, M. Changes in brain function of depressed subjects during treatment with placebo. *Am. J. Psychiatry* **159**, 122–129 (2002).
91. Graversen, C. et al. The analgesic effect of pregabalin in patients with chronic pain is reflected by changes in pharmaco-EEG spectral indices. *Br. J. Clin. Pharmacol.* **73**, 363–372 (2012).
92. He, F. et al. Effects of 20 Hz repetitive transcranial magnetic stimulation on disorders of consciousness: a resting-state electroencephalography study. *Neural Plast.* **2018**, 5036184 (2018).
93. Liu, M. et al. Effects of transcranial direct current stimulation on EEG power and brain functional network in stroke patients. *IEEE Trans. Neural Syst. Rehabil. Eng.* **31**, 335–345 (2023).
94. Li, L. et al. Placebo analgesia changes alpha oscillations induced by tonic muscle pain: EEG frequency analysis including data during pain evaluation. *Front Comput Neurosci.* <https://doi.org/10.3389/fncom.2016.00045> (2016).
95. Huneke, N. T. M. et al. Experimental placebo analgesia changes resting-state alpha oscillations. *PLoS ONE* <https://doi.org/10.1371/journal.pone.0078278> (2013).
96. Corrigan, J. D. & Bogner, J. Initial reliability and validity of the Ohio State University TBI identification method. *J. Head Trauma Rehabil.* **22**, 318–329 (2007).
97. Ona, G. et al. The adverse events of ibogaine in humans: an updated systematic review of the literature (2015–2020). *Psychopharmacology* **239**, 1977–1987 (2022).
98. Alper, K. R. Ibogaine: a review. In *The Alkaloids: Chemistry and Biology* Vol 56, 1–38 (Academic Press, 2001); [https://doi.org/10.1016/S0099-9598\(01\)56005-8](https://doi.org/10.1016/S0099-9598(01)56005-8)
99. Montgomery, S. A. & Asberg, M. A new depression scale designed to be sensitive to change. *Br. J. Psychiatry* **134**, 382–389 (1979).
100. Wechsler, D. *Wechsler Adult Intelligence Scale* 4th edn (Pearson, 2008); <https://www.pearsonassessments.com/store/usassessments/en/Store/Professional-Assessments/Cognition-%26-Neuro/Wechsler-Adult-Intelligence-Scale-%7C-Fourth-Edition/p/100000392.html>
101. Conners, C. K. *Conners Continuous Performance Test Third Edition* (MHS, 2014); <https://storefront.mhs.com/collections/conners-cpt-3>
102. Harris, P. A. et al. Research electronic data capture (REDCap)—a metadata-driven methodology and workflow process for providing translational research informatics support. *J. Biomed. Inform.* **42**, 377–381 (2009).
103. Duan, W. et al. Reproducibility of power spectrum, functional connectivity and network construction in resting-state EEG. *J. Neurosci. Methods* **348**, 108985 (2021).
104. Gudmundsson, S., Runarsson, T. P., Sigurdsson, S., Eiriksdottir, G. & Johnsen, K. Reliability of quantitative EEG features. *Clin. Neurophysiol.* **118**, 2162–2171 (2007).
105. Rolle, C. E. et al. Functional connectivity using high density EEG shows competitive reliability and agreement across test/retest sessions. *J. Neurosci. Methods* **367**, 109424 (2022).
106. Popov, T. et al. Test–retest reliability of resting-state EEG in young and older adults. *Psychophysiology* **60**, e14268 (2023).
107. Delorme, A. & Makeig, S. EEGLAB: an open source toolbox for analysis of single-trial EEG dynamics including independent component analysis. *J. Neurosci. Methods* **134**, 9–21 (2004).
108. Wu, W. et al. ARTIST: a fully automated artifact rejection algorithm for single-pulse TMS-EEG data. *Hum. Brain Mapp.* **39**, 1607–1625 (2018).
109. Bell, A. J. & Sejnowski, T. J. An information-maximization approach to blind separation and blind deconvolution. *Neural Comput.* **7**, 1129–1159 (1995).
110. Haegens, S., Cousijn, H., Wallis, G., Harrison, P. J. & Nobre, A. C. Inter- and intra-individual variability in alpha peak frequency. *Neuroimage* **92**, 46–55 (2014).
111. Klimesch, W., Sauseng, P. & Gerloff, C. Enhancing cognitive performance with repetitive transcranial magnetic stimulation at human individual alpha frequency. *Eur. J. Neurosci.* **17**, 1129–1133 (2003).
112. Roelofs, C. L. et al. Individual alpha frequency proximity associated with repetitive transcranial magnetic stimulation outcome: An independent replication study from the ICON-DB consortium. *Clin. Neurophysiol.* **132**, 643–649 (2021).
113. Tadel, F., Baillet, S., Mosher, J. C., Pantazis, D. & Leahy, R. M. Brainstorm: a user-friendly application for MEG/EEG analysis. *Comput. Intell. Neurosci.* **2011**, 879716 (2011).
114. Hauk, O. Keep it simple: a case for using classical minimum norm estimation in the analysis of EEG and MEG data. *Neuroimage* **21**, 1612–1621 (2004).

115. Trivedi, M. H. et al. Establishing moderators and biosignatures of antidepressant response in clinical care (EMBARC): rationale and design. *J. Psychiatr. Res.* **78**, 11–23 (2016).
116. Schartner, M. et al. Complexity of multi-dimensional spontaneous EEG decreases during propofol induced general anaesthesia. *PLoS ONE* <https://doi.org/10.1371/journal.pone.0133532> (2015).
117. Theiler, J., Eubank, S., Longtin, A., Galdrikian, B. & Doynne Farmer, J. Testing for nonlinearity in time series: the method of surrogate data. *Phys. Nonlinear Phenom.* **58**, 77–94 (1992).
118. Delorme, A. et al. EEGLAB, SIFT, NFT, BCILAB, and ERICA: new tools for advanced EEG processing. *Comput. Intell. Neurosci.* **2011**, 130714 (2011).
119. Franke, L. M., Perera, R. A. & Sponheim, S. R. Long-term resting EEG correlates of repetitive mild traumatic brain injury and loss of consciousness: alterations in alpha-beta power. *Front. Neurol.* **14**, 1241481 (2023).
120. Bazanova, O. M. & Vernon, D. Interpreting EEG alpha activity. *Neurosci. Biobehav. Rev.* **44**, 94–110 (2014).
121. Dunnett, C. W. A multiple comparison procedure for comparing several treatments with a control. *J. Am. Stat. Assoc.* **50**, 1096–1121 (1955).
122. Maris, E. & Oostenveld, R. Nonparametric statistical testing of EEG- and MEG-data. *J. Neurosci. Methods* **164**, 177–190 (2007).

Acknowledgements

We thank the veterans who participated in this study. This work was made possible by the generous donations of S. and G. Jurvetson, the Effie and Wofford Cain Foundation, E. Jhong, the Saisei Foundation, L. Keller, and by support from and collaboration with Veterans Exploring Treatment Solutions (VETS), Inc., a nonprofit organization committed to advancing health-care options for veterans. This work was also supported by Canadian Institutes of Health Research Fellowships (176536 to J.I.L. and 181910 to D.B.). The funders had no role in study design, data collection and analysis, decision to publish or preparation of the manuscript. For their support on the project, we also thank N. Johnson, M. Mattos, S. Hunegnaw, T. Dinh, A. Geoly, L. Anker, O. Keynan, A. Faerman, B. Wong, A. Shamma and T.J. Ford.

Author contributions

J.I.L. and A.C. performed data preprocessing and analyses, created all visualizations and wrote the manuscript. J.I.L., K.N.C. and N.R.W. were responsible for EEG study design. K.N.C. performed screening, psychological and cognitive assessments and supervised related scoring and data entry, and led study execution at Stanford for all participants. D.B. and F.E. contributed to interpretation of the data. J.N.K. and C.E.R. contributed to supervision of the research and interpretation of the data. M. Sridhar contributed to data acquisition and interpretation of the data. M. Saggat contributed to data analysis

and interpretation of the data. C.J.K. contributed to data analysis, supervised the EEG analyses and contributed to interpretation of the data. N.R.W. conceived the study, acquired funding for the study, supervised study design, budgeting and execution at Stanford, and was protocol director of the study. All authors contributed to the review and editing of the manuscript and approved the final manuscript.

Competing interests

C.J.K. holds equity in Alto Neuroscience, Inc and is a consultant for Flow Neuroscience. N.R.W. is a named inventor on Stanford-owned intellectual property relating to magnesium–ibogaine; he has served on scientific advisory boards for Otsuka, NeuraWell, Magnus Medical, Soneira and Nooma as a paid adviser, and he has equity/stock options in NeuraWell, Soneira and Nooma. N.R.W. and J.I.L. are listed as inventors on US provisional patent applications that cover some of the aspects reported here (63/804,501). The remaining authors declare no competing interests.

Additional information

Extended data are available for this paper at <https://doi.org/10.1038/s44220-025-00463-x>.

Supplementary information The online version contains supplementary material available at <https://doi.org/10.1038/s44220-025-00463-x>.

Correspondence and requests for materials should be addressed to Nolan R. Williams.








Peer review information *Nature Mental Health* thanks Joel Frohlich, Marc Nuwer and Enzo Tagliazucchi for their contribution to the peer review of this work.

Reprints and permissions information is available at www.nature.com/reprints.

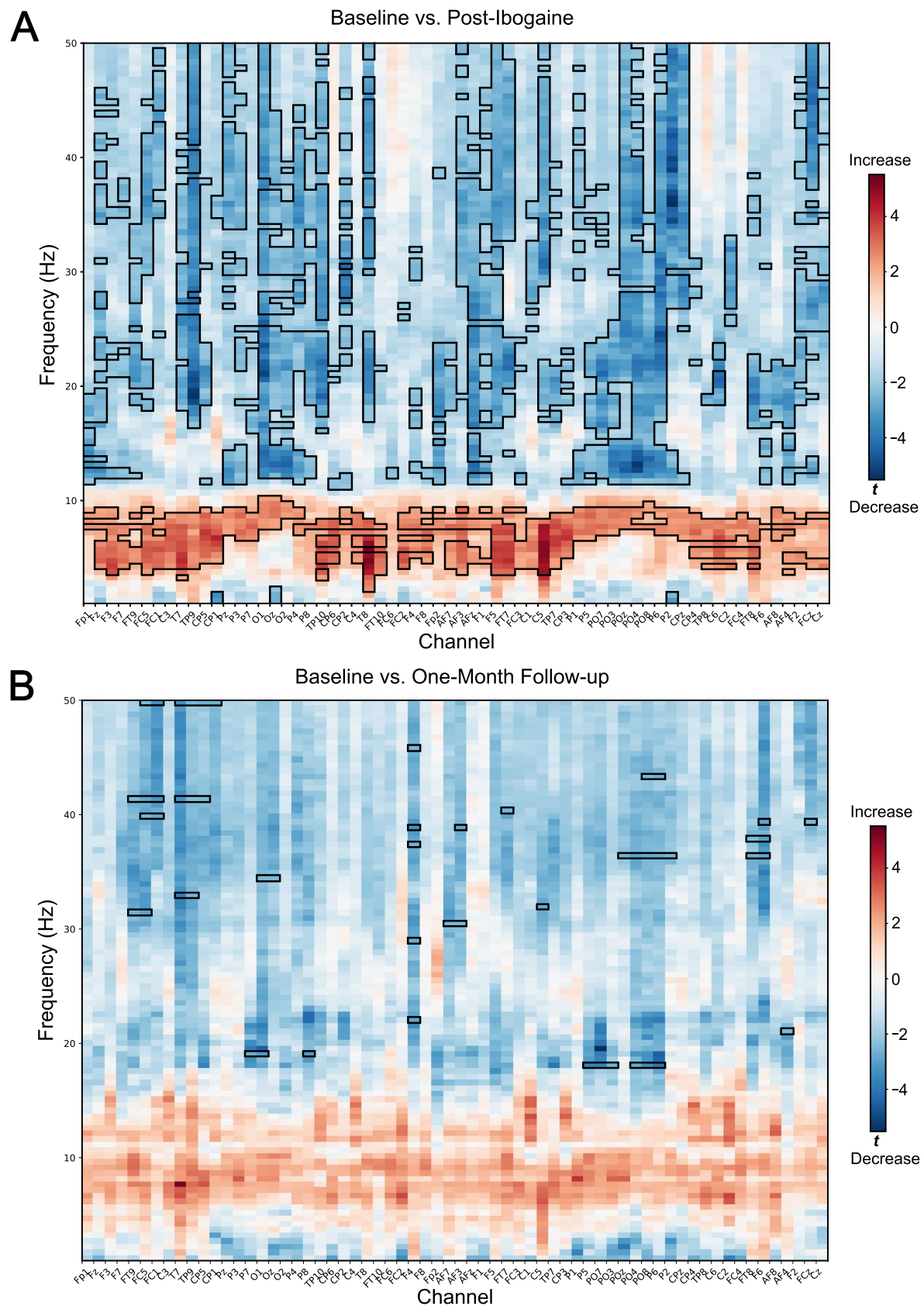
Publisher's note Springer Nature remains neutral with regard to jurisdictional claims in published maps and institutional affiliations.

Springer Nature or its licensor (e.g. a society or other partner) holds exclusive rights to this article under a publishing agreement with the author(s) or other rightsholder(s); author self-archiving of the accepted manuscript version of this article is solely governed by the terms of such publishing agreement and applicable law.

© The Author(s), under exclusive licence to Springer Nature America, Inc. 2025

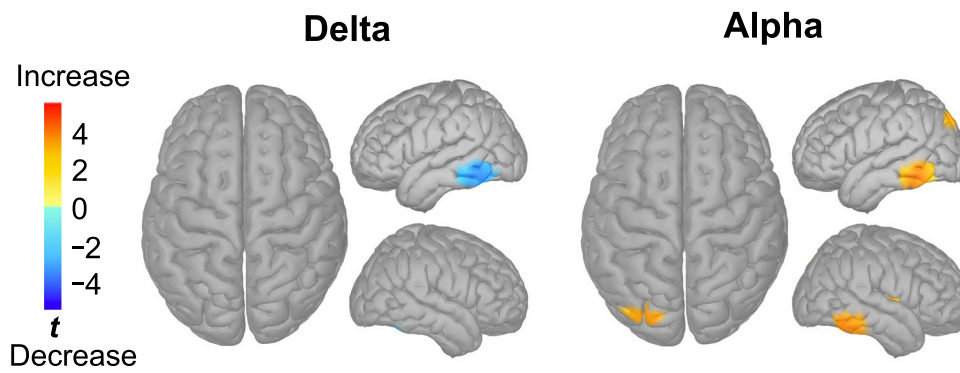
Jennifer I. Lissemore ^{1,4}, **Anna Chaiken**^{1,4}, **Kirsten N. Cherian** ¹, **Derrick Buchanan** ¹, **Flint Espil**¹, **Jackob N. Keynan**¹, **Malvika Sridhar** ¹, **Camarin E. Rolle**¹, **Manish Saggat** ¹, **Corey J. Keller** ^{1,2,3,5} & **Nolan R. Williams** ^{1,5} ✉

¹Department of Psychiatry and Behavioral Sciences, Stanford University Medical Center, Stanford, CA, USA. ²Wu Tsai Neurosciences Institute, Stanford University, Stanford, CA, USA. ³Sierra Pacific Mental Illness, Research, Education and Clinical Center (MIRECC), Veterans Affairs Palo Alto Healthcare System, Palo Alto, CA, USA. ⁴These authors contributed equally: Jennifer I. Lissemore, Anna Chaiken. ⁵These authors jointly supervised this work: Corey J. Keller, Nolan R. Williams. ✉ e-mail: nolanw@stanford.edu



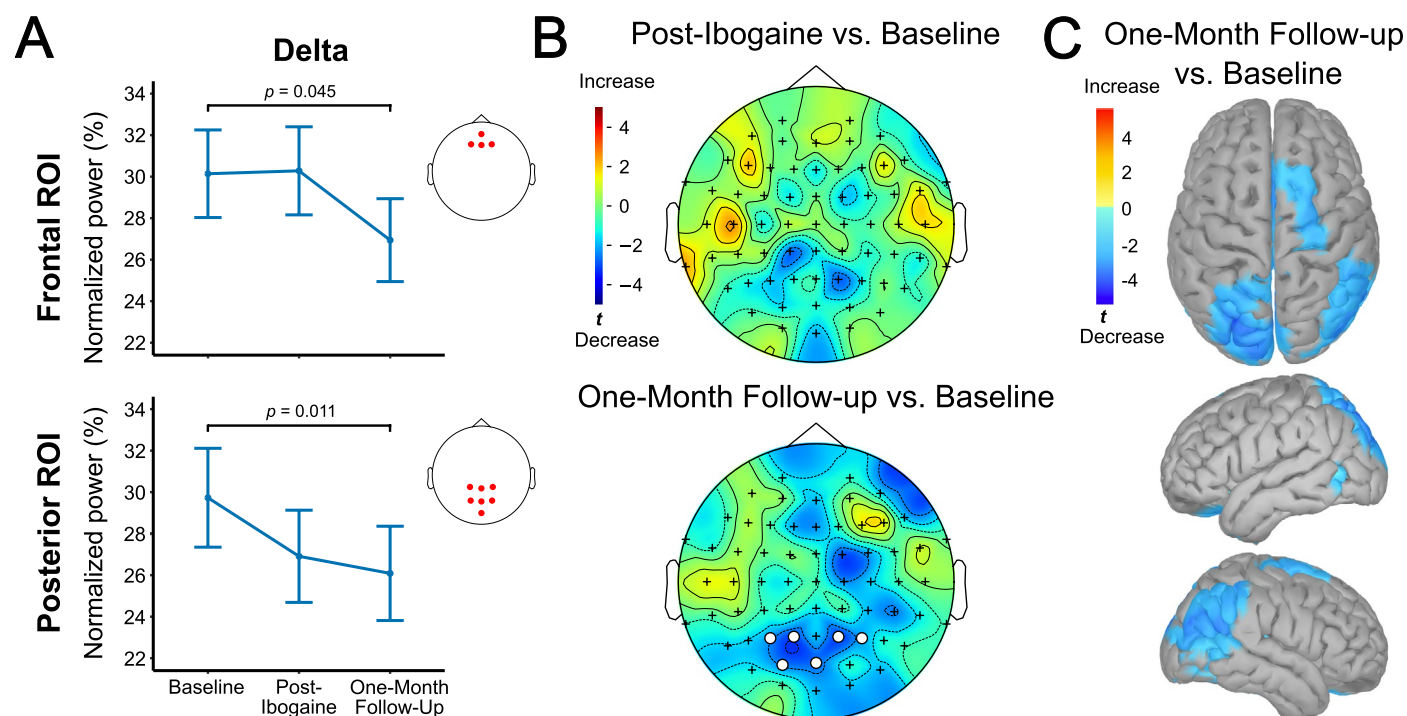
Extended Data Fig. 1 | Cluster-based permutation test results, showing changes in normalized power at the sensor level across 1–50 Hz and 64 channels from baseline to post-ibogaine (a) and one-month follow-up (b). Significant clusters are highlighted with a black border. All clusters $p \leq 0.05$.

Changes in Power After 1 Week of Placebo vs. Baseline



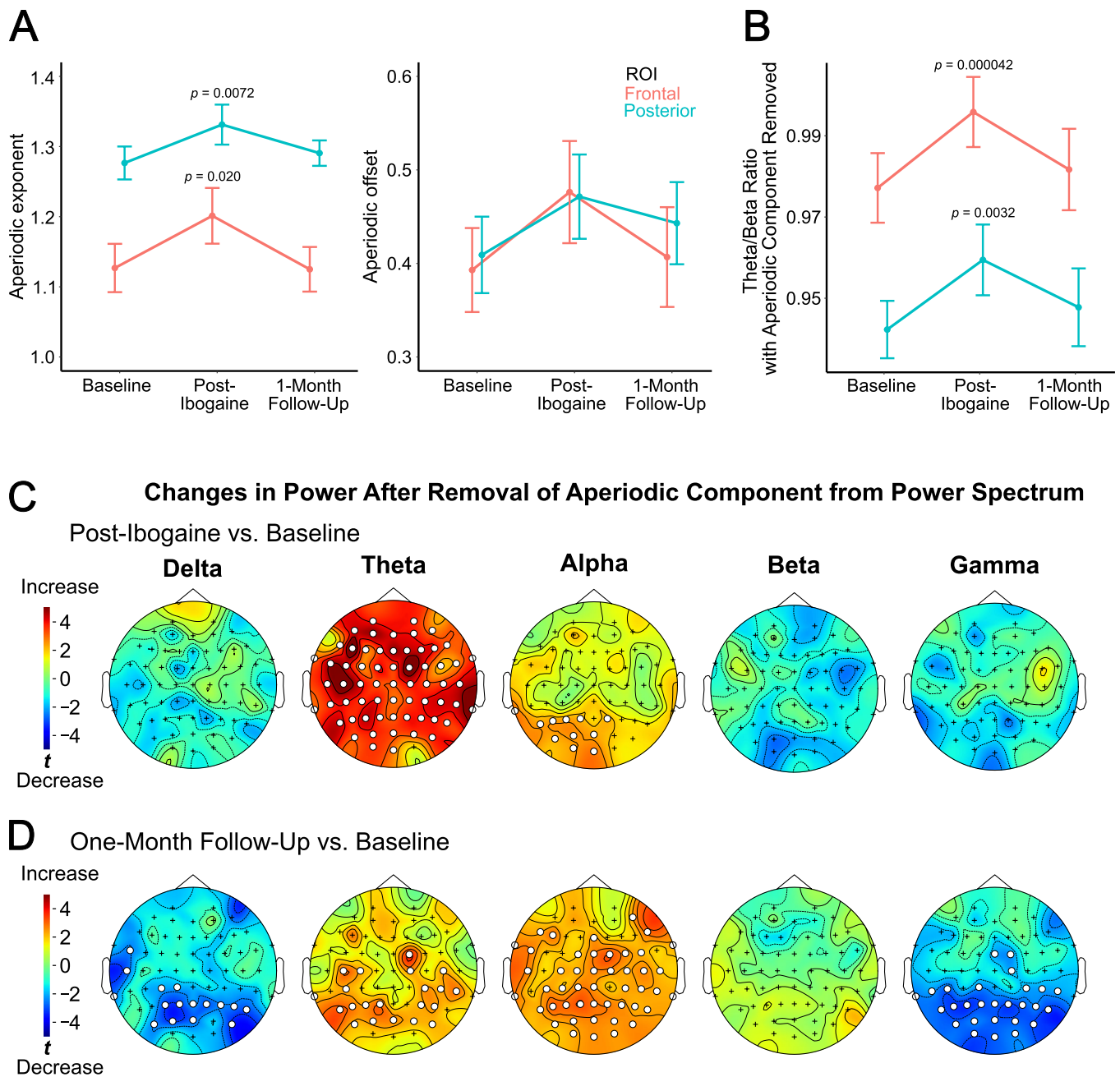
Extended Data Fig. 2 | Changes in normalized power in source space after one week of placebo intervention in an age-matched subset of patients with depression from the EMBARC trial. Source estimation localized placebo effects on delta power to left interior temporal cortex, and placebo effects on alpha

power to bilateral middle and temporal cortices and left parietal cortex ($n = 30$). Significant clusters reflect $p_{\text{FDR}} < 0.05$. No significant placebo effects were observed for theta, beta, or gamma power.



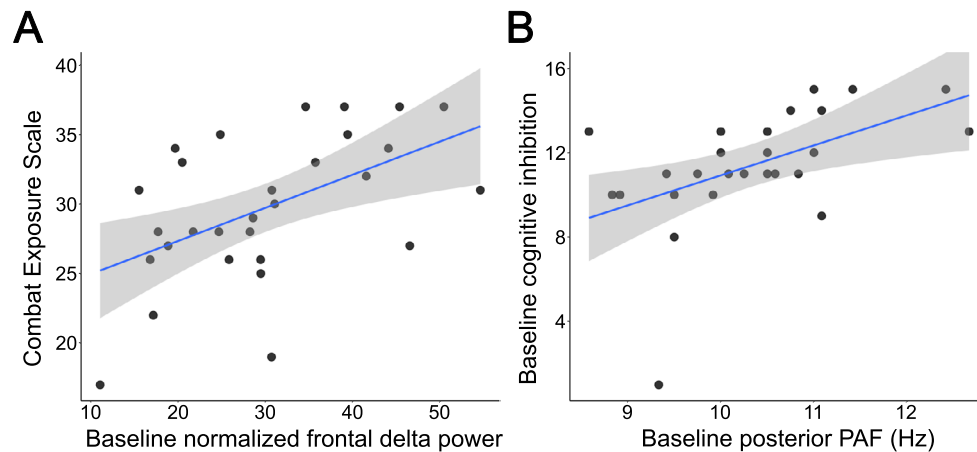
Extended Data Fig. 3 | Reduced delta power one month after ibogaine treatment. **a.** In predefined frontal and posterior regions of interest (ROIs), delta power decreased significantly one month after ibogaine, as compared to baseline (post-ibogaine $n = 30$, 1-month follow-up $n = 26$; Dunnett's test, two-sided). Error bars represent standard error of the mean. **b.** Channel-wide cluster-based permutation tests comparing normalized delta power at baseline vs.

post-ibogaine (top) or 1-month follow-up (bottom) at the sensor level similarly revealed reduced delta power at one-month follow-up. Significant clusters are displayed as white circles. **c.** Source estimation localized 1-month reductions in delta power to parietal and right superior frontal cortical regions (without FDR correction for multiple comparisons).



Extended Data Fig. 4 | Changes in aperiodic and periodic components after ibogaine treatment. a. The aperiodic exponent in frontal and posterior ROIs increased significantly post-ibogaine compared to baseline ($n = 30$; Dunnett's test, two-sided). **b.** After removal of the aperiodic component from the power spectrum, significant increases in the theta/beta ratio post-ibogaine persisted in both ROIs ($n = 30$; Dunnett's test, two-sided). Error bars represent the standard error of the mean. **c.** Topoplots of cluster-based permutation test results show

that after removal of the aperiodic component from the power spectrum, theta and alpha power increase significantly post-ibogaine compared to baseline ($n = 30$). No significant clusters were identified post-ibogaine for delta, beta, and gamma power ($n = 30$). **d.** Using the flattened spectrum, significant decreases in delta and gamma power, and significant increases in theta and alpha power were observed at one-month follow-up compared to baseline ($n = 27$). Significant clusters (two-tailed $p < 0.05$) are displayed as white circles.



Extended Data Fig. 5 | Pre-treatment associations between 'slowing' of cortical rhythms and indices of TBI pathology. To explore whether baseline indices of TBI pathology were related to the slowing of cortical rhythms before ibogaine treatment, additional correlations were performed between EEG measures at baseline and combat exposure, number of TBIs, and symptom severity at baseline. Exploratory correlations were performed with Spearman's rho, using a statistical threshold of $p < 0.005$ to control type I and type II errors. **a.** Higher frontal delta power prior to treatment showed a significant correlation with greater combat exposure (frontal ROI: $\rho = 0.51$, $p = 0.0048$). Baseline posterior delta power showed a similar but non-significant correlation with combat

exposure (posterior ROI: $\rho = 0.33$, $p = 0.071$). **b.** Lower peak alpha frequency (PAF) prior to treatment showed a significant correlation with poorer baseline cognitive inhibition (global PAF: $\rho = 0.59$, $p = 0.0015$; posterior PAF: $\rho = 0.59$, $p = 0.0016$). All other baseline correlations were non-significant. The observed associations may be consistent with TBI pathology involving 'slowing' of cortical rhythms. However, demonstration of abnormal 'slowing' of cortical rhythms at baseline at the group level would require comparisons with an age-matched control group. For visualization purposes, the blue line represents a linear model fit, and the shaded grey area represents the 95% confidence intervals.

Reporting Summary

Nature Portfolio wishes to improve the reproducibility of the work that we publish. This form provides structure for consistency and transparency in reporting. For further information on Nature Portfolio policies, see our [Editorial Policies](#) and the [Editorial Policy Checklist](#).

Statistics

For all statistical analyses, confirm that the following items are present in the figure legend, table legend, main text, or Methods section.

- | | |
|-------------------------------------|--|
| n/a | Confirmed |
| <input type="checkbox"/> | <input checked="" type="checkbox"/> The exact sample size (<i>n</i>) for each experimental group/condition, given as a discrete number and unit of measurement |
| <input type="checkbox"/> | <input checked="" type="checkbox"/> A statement on whether measurements were taken from distinct samples or whether the same sample was measured repeatedly |
| <input type="checkbox"/> | <input checked="" type="checkbox"/> The statistical test(s) used AND whether they are one- or two-sided
<i>Only common tests should be described solely by name; describe more complex techniques in the Methods section.</i> |
| <input type="checkbox"/> | <input checked="" type="checkbox"/> A description of all covariates tested |
| <input type="checkbox"/> | <input checked="" type="checkbox"/> A description of any assumptions or corrections, such as tests of normality and adjustment for multiple comparisons |
| <input type="checkbox"/> | <input checked="" type="checkbox"/> A full description of the statistical parameters including central tendency (e.g. means) or other basic estimates (e.g. regression coefficient) AND variation (e.g. standard deviation) or associated estimates of uncertainty (e.g. confidence intervals) |
| <input type="checkbox"/> | <input checked="" type="checkbox"/> For null hypothesis testing, the test statistic (e.g. <i>F</i> , <i>t</i> , <i>r</i>) with confidence intervals, effect sizes, degrees of freedom and <i>P</i> value noted
<i>Give P values as exact values whenever suitable.</i> |
| <input checked="" type="checkbox"/> | <input type="checkbox"/> For Bayesian analysis, information on the choice of priors and Markov chain Monte Carlo settings |
| <input checked="" type="checkbox"/> | <input type="checkbox"/> For hierarchical and complex designs, identification of the appropriate level for tests and full reporting of outcomes |
| <input type="checkbox"/> | <input checked="" type="checkbox"/> Estimates of effect sizes (e.g. Cohen's <i>d</i> , Pearson's <i>r</i>), indicating how they were calculated |

Our web collection on [statistics for biologists](#) contains articles on many of the points above.

Software and code

Policy information about [availability of computer code](#)

Data collection	Data were collected in REDCap and using BrainVision Recorder.
Data analysis	The Matlab EEGLAB toolbox used for pre-processing and sensor-space spectral measures can be downloaded from https://scn.ucsd.edu/eeglab/download.php . ROI-based statistical analyses were performed using R version 4.3.1 (in RStudio v.2023.06.0) publicly available packages readxl v.1.4.2, lmerTest v.3.1-3, emmeans v.1.8.7, and rstatix v.0.7.2. Cluster-based permutation tests were performed using the freely available python MNE toolbox (mne.stats.permutation_cluster_1samp_test). Source estimation was performed using MATLAB Brainstorm, which is freely available (https://neuroimage.usc.edu/bst/download.php). Lempel-Ziv complexity measures were computed using publicly available code from Shartner et al. 2015 (https://doi.org/10.1371/journal.pone.0133532.s002) and the SIFT EEGLAB plugin (https://github.com/scn/SIFT/blob/master/stat/stat_surrogateGen.m). The FOOF toolbox v1.1 for calculating aperiodic components of the EEG signal is publicly available (https://foof-tools.github.io/foof/). Other scripts used to analyze the data of this study are available at https://github.com/achaiken/lbogaine_rsEEG_project .

For manuscripts utilizing custom algorithms or software that are central to the research but not yet described in published literature, software must be made available to editors and reviewers. We strongly encourage code deposition in a community repository (e.g. GitHub). See the Nature Portfolio [guidelines for submitting code & software](#) for further information.

Data

Policy information about [availability of data](#)

All manuscripts must include a [data availability statement](#). This statement should provide the following information, where applicable:

- Accession codes, unique identifiers, or web links for publicly available datasets
- A description of any restrictions on data availability
- For clinical datasets or third party data, please ensure that the statement adheres to our [policy](#)

Owing to the sensitivity of psychiatric patient data, our IRB requires individualized review before data sharing. We have produced anonymized data related to the present findings for sharing with all scientists with research and data safeguarding plans that comport with Stanford University guidelines. Anonymized data sharing does not require the use of a data use agreement. Please contact N. Williams at nolanw@stanford.edu with data-sharing requests with an approximate response time within 90 days. Data from EMBARC are publicly available and can be accessed upon request here: https://nda.nih.gov/edit_collection.html?id=2199

Research involving human participants, their data, or biological material

Policy information about studies with [human participants or human data](#). See also policy information about [sex, gender \(identity/presentation\), and sexual orientation](#) and [race, ethnicity and racism](#).

Reporting on sex and gender

All participants self identified as male. Gender or biological sex was not used for analysis purposes. Gender was determined by the participants using classification terms provided by the researchers. Classification terms were: "male", "female", or "other".

Reporting on race, ethnicity, or other socially relevant groupings

Reported in Table S1.

Population characteristics

Reported in Table S1 and the Methods section.

Recruitment

Participants were referred to the study by VETS, Inc. after being approved for a treatment grant. Veterans who were assessed by VETS as requiring treatment acutely were not referred to the study. As described in the online methods, participants were SOV who had independently scheduled themselves for MISTIC. As detailed in the discussion section, the study was not controlled, and so the relative contribution of this potential bias to the observed effects cannot be determined. Supplementary analysis of placebo effects on EEG measures from the publicly available EMBARC study indicated that many of the observed EEG changes were not likely driven by placebo effects, however.

Ethics oversight

All research procedures were approved by Stanford University Institutional Review Board, and all participants provided written informed consent.

Note that full information on the approval of the study protocol must also be provided in the manuscript.

Field-specific reporting

Please select the one below that is the best fit for your research. If you are not sure, read the appropriate sections before making your selection.

☐ Life sciences ☒ Behavioural & social sciences ☐ Ecological, evolutionary & environmental sciences

For a reference copy of the document with all sections, see nature.com/documents/nr-reporting-summary-flat.pdf

Behavioural & social sciences study design

All studies must disclose on these points even when the disclosure is negative.

Study description

This was a prospective, single-arm, observational study of ibogaine treatment, assessing the effects of treatment on resting-state electroencephalography (EEG) data that were collected at baseline, immediately after, and one month after treatment. Analysis was quantitative.

Research sample

Study population consisted of 30 US special operations veterans (aged 18-70; all males) with a history of traumatic brain injury. The study sample is representative of Special Operation Veterans (SOV). SOV was selected as the target population considering the high burden and prevalence of TBI.

Sampling strategy

This is a convenience sample. Clinician administered scales were collected by a neuropsychologist and logged in REDcap. Self report scales were independently logged by the participant using a REDcap instrument. As an observational study, no power calculation was performed. Sample size of 30 was selected to balance our desire for a larger sample with the importance of providing prompt preliminary safety and efficacy data to other SOV who are considering this treatment given their potentially vulnerable status. Using G*Power v.3.1, a post hoc power analysis based on the average effect size (Cohen's $d = 0.64$) observed across EEG measures for baseline to post-ibogaine comparisons indicated that the study achieved 92.3% power with a sample size of 30 participants. This suggests that the study was adequately powered to detect medium-to-large effects.

Data collection	Recruitment took place between November 2021 to September 2022. EEG data were recorded using an actiCAP slim EEG cap (Brain Products GmbH, Germany) with 64 Ag-AgCl channels, and an acti64CHamp Amplifier. Clinical interviews were conducted via Zoom or in person at Stanford University. Neuropsychological assessments were conducted in person at Stanford University. Clinician administered scales were collected by a neuropsychologist and logged in REDcap. Self report scales were independently logged by the participant using a REDcap instrument. Participants were assessed individually by research staff, and assessments were video recorded with participant consent. Clinician-administered scales were collected by a neuropsychologist and logged in REDCap. Self-report scales were independently logged by the participant using a REDCap instrument. As the study was open-label, the researchers were not blinded to experimental conditions or study hypotheses, except during EEG data preprocessing, which was performed by an experienced rater who was blind to the visit number and clinical scores associated with each recording.
Timing	November 2021 to September 2022
Data exclusions	No enrolled participants were excluded from the primary analyses.
Non-participation	34 participants were screened before enrollment. One did not meet study inclusion criteria. 33 participants were initially enrolled; 2 participants were withdrawn due to not meeting the study inclusion criteria, and one participant was withdrawn due to acute substance use withdrawal symptoms. No participants dropped out/declined participation.
Randomization	The trial was not randomized. Relevant covariates (age, combat exposure score, and total number of TBIs) were controlled for by including them as covariates in the LME models (primary analysis). All participants were male, therefore sex did not need to be considered as a covariate.

Reporting for specific materials, systems and methods

We require information from authors about some types of materials, experimental systems and methods used in many studies. Here, indicate whether each material, system or method listed is relevant to your study. If you are not sure if a list item applies to your research, read the appropriate section before selecting a response.

Materials & experimental systems

- n/a | Involved in the study
- ☒ ☐ Antibodies
- ☒ ☐ Eukaryotic cell lines
- ☒ ☐ Palaeontology and archaeology
- ☒ ☐ Animals and other organisms
- ☐ ☒ Clinical data
- ☒ ☐ Dual use research of concern
- ☒ ☐ Plants

Methods

- n/a | Involved in the study
- ☒ ☐ ChIP-seq
- ☒ ☐ Flow cytometry
- ☒ ☐ MRI-based neuroimaging

Clinical data

Policy information about [clinical studies](#)

All manuscripts should comply with the ICMJE [guidelines for publication of clinical research](#) and a completed [CONSORT checklist](#) must be included with all submissions.

Clinical trial registration	NCT04313712
Study protocol	https://doi.org/10.1038/s41591-023-02705-w
Data collection	Data was collected at Stanford University as well as remotely via secure virtual platform between November 2021 to September 2022.
Outcomes	Associations between EEG measures and clinical outcome measures were investigated. Clinical outcomes of interest were: improvements in the Clinician Administered PTSD Scale (CAPS-5), Montgomery-Åsberg Depression Rating Scale (MADRS), and Hamilton-Anxiety Rating Scale (HAM-A) one month after treatment. Associations with EEG measures were assessed using Spearman's rho.

Seed stocks

Report on the source of all seed stocks or other plant material used. If applicable, state the seed stock centre and catalogue number. If plant specimens were collected from the field, describe the collection location, date and sampling procedures.

Novel plant genotypes

Describe the methods by which all novel plant genotypes were produced. This includes those generated by transgenic approaches, gene editing, chemical/radiation-based mutagenesis and hybridization. For transgenic lines, describe the transformation method, the number of independent lines analyzed and the generation upon which experiments were performed. For gene-edited lines, describe the editor used, the endogenous sequence targeted for editing, the targeting guide RNA sequence (if applicable) and how the editor was applied.

Authentication

Describe any authentication procedures for each seed stock used or novel genotype generated. Describe any experiments used to assess the effect of a mutation and, where applicable, how potential secondary effects (e.g. second site T-DNA insertions, mosaicism, off-target gene editing) were examined.